Supplementary Data

A novel tetrathiafulvalene based liquid crystalline organogelator: synthesis, self-assembly properties and potential utilization

Chao Xu,[a,b] Li Wang,[a,b] Yan Xia,[a,b] Dongfeng Li,[a] Bingzhu Yin*[c] and Ruibin Hou *[a,b]

[a] *School of Chemistry and Life Science, Changchun University of Technology, Changchun, Jilin 130012, PR China*

[b] *Advanced Institute of Materials Science, Changchun University of Technology, Changchun, Jilin 130012, PR China*

[c] *Key Laboratory of Natural Resources of Changbai Mountain & Functional Molecules, Yanbian University, Ministry of Education, Yanji, Jilin 133002, PR China*

1. Instrumentation

NMR experiments

All solution state NMR studies were carried out on Bruker AV-400 Spectrometer (400 MHz for ^{1}H and 75 MHz for ^{13}C) and chemical shifts were referenced relative to tetramethylsilane (δ_H/δ_C=0).

FT-IR spectroscopy

IR spectra were recorded on a Nicolet iS 50 FT-IR instrument with the KBr disk technique.

MALDI-TOF-MS spectrometry

MALDI-TOF-MS was performed on a Bruker autoflexIII using a 1,8,9-anthracenetriol (DITH) matrix.

Small-angle X-ray diffracting

Small-angle X-ray scattering (SAXS) measurements were carried out at 298 K on a beam line 1W2A synchrotron radiation X-ray small angle system at Beijing Synchrotron Radiation Facility (λ =1.54Å).

From the experimental values of the unit cell parameters (*a*, *b*, *c*, and γ) and the density (ρ), the average number of molecules per cross-sectional slice of the column can be calculated according to Eq 1, where M is the molecular mass and NA is Avogadro's number

$$n = abc\rho N_A \sin\gamma / M \qquad \text{Eq S1.}$$

Scanning electron microscope (SEM)

The gel samples were placed on a silicon wafer, and dried for a couple of hours under room temperature before imaging. A layer of gold was sputtered on top to form a conducting surface

and finally the specimen was transferred into a Field Emission Scanning Electron Microscope (JEOL7610 FE-SEM).

^{1}H, ^{13}C NMR, IR and MALDI-TOF-MS Spectra

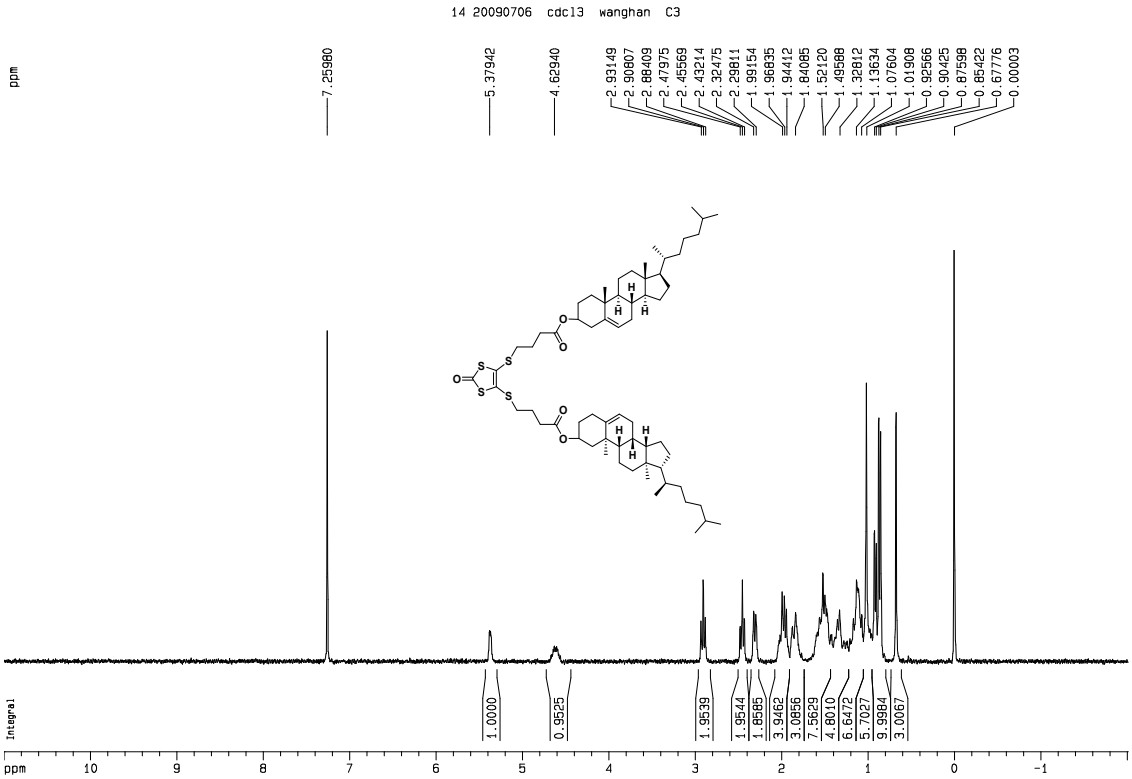

Fig. S1 ^{1}H NMR of derivative **3a**

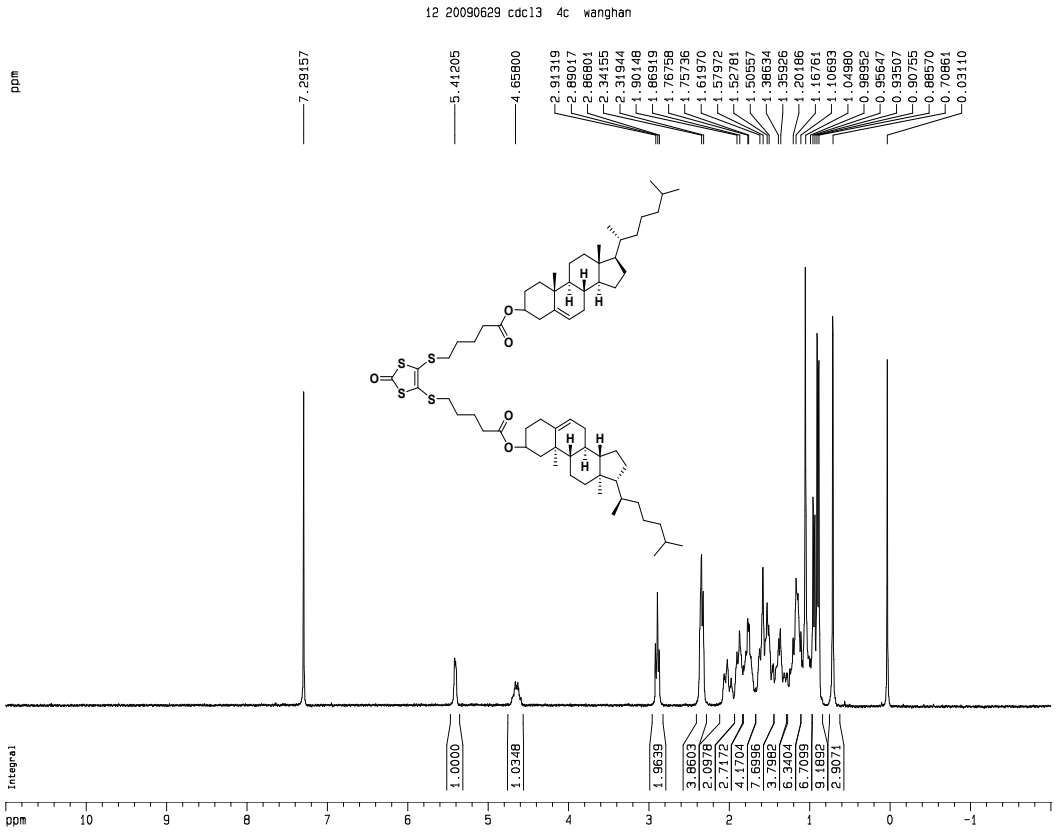

Fig. S2 ^{1}H NMR of derivative **3b**

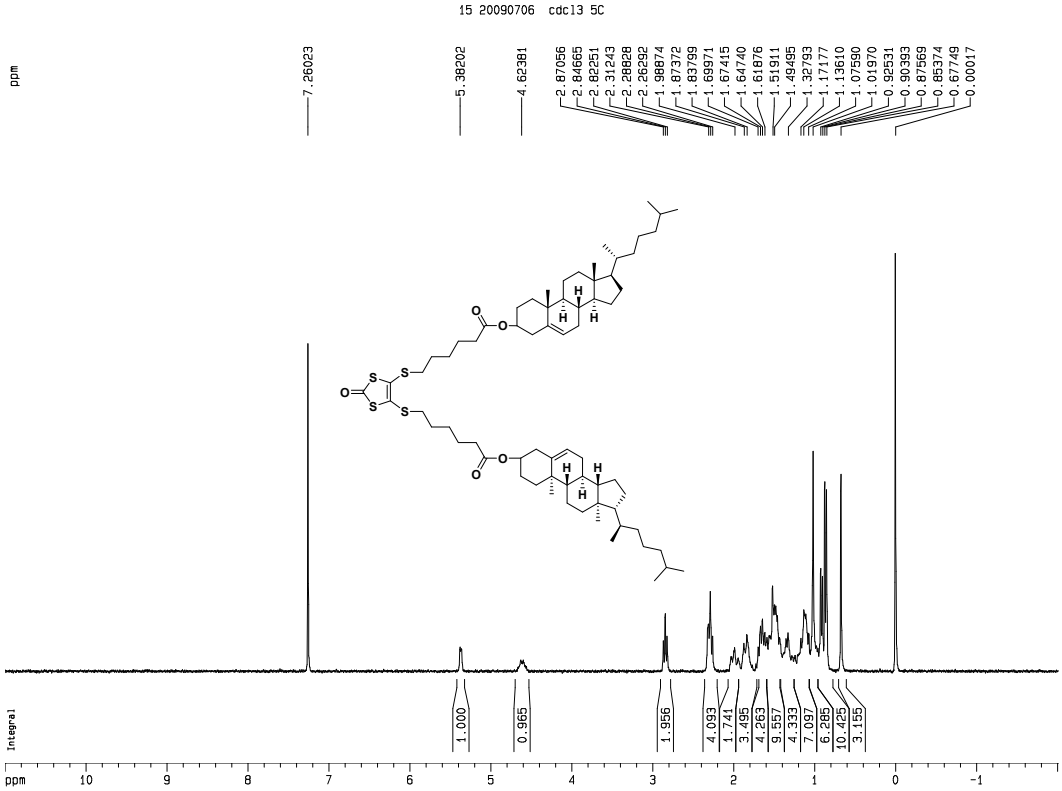

Fig. S3 ^{1}H NMR of derivative **3c**

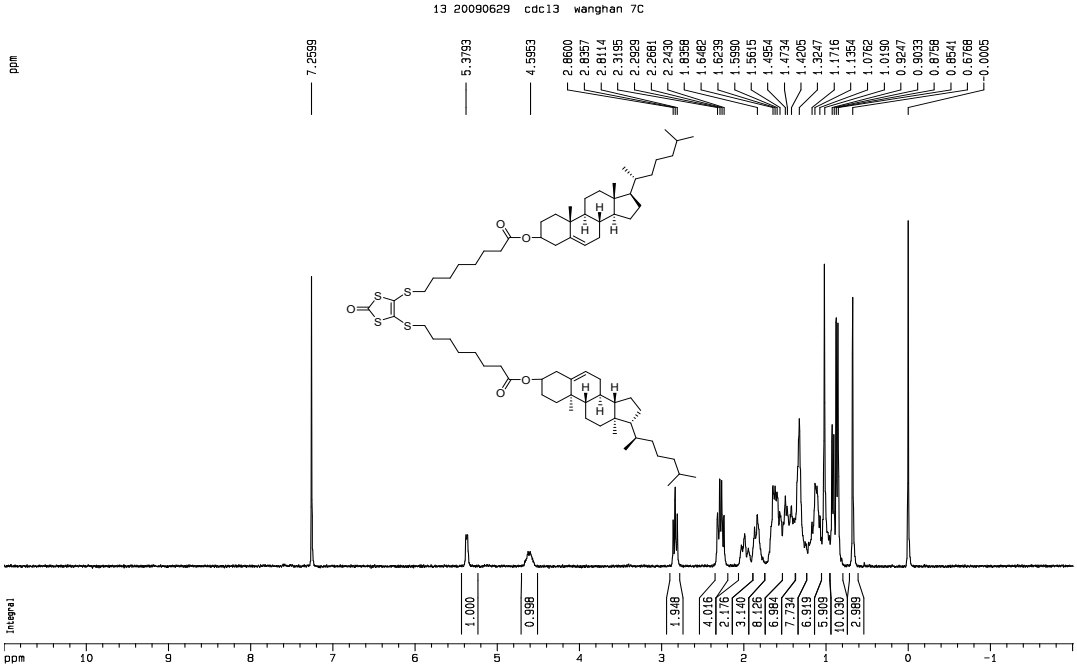

Fig. S4 ^{1}H NMR of derivative **3d**

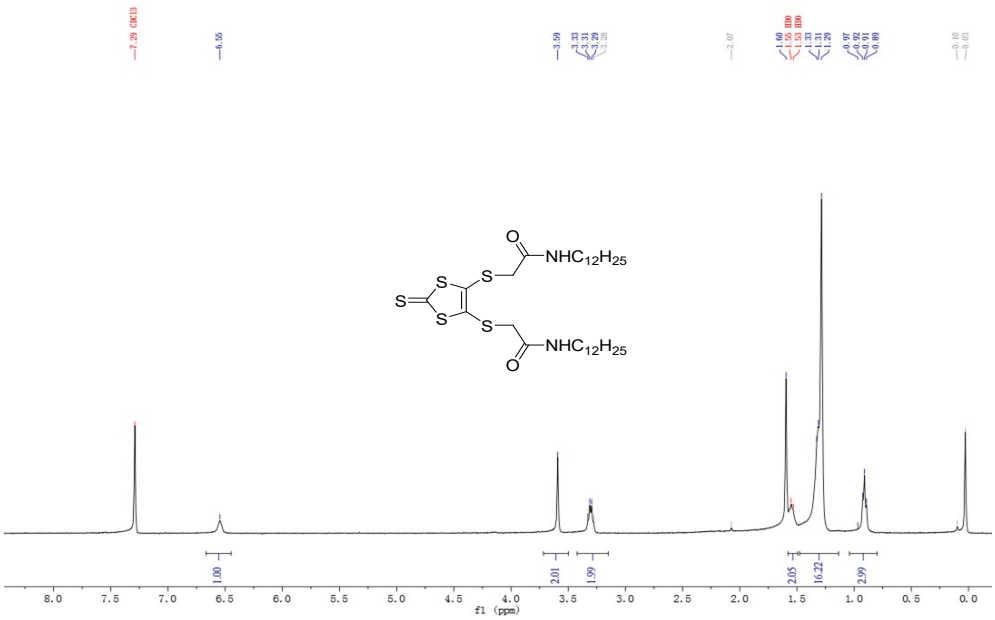

Fig. S5 ^{1}H NMR of derivative **2a**

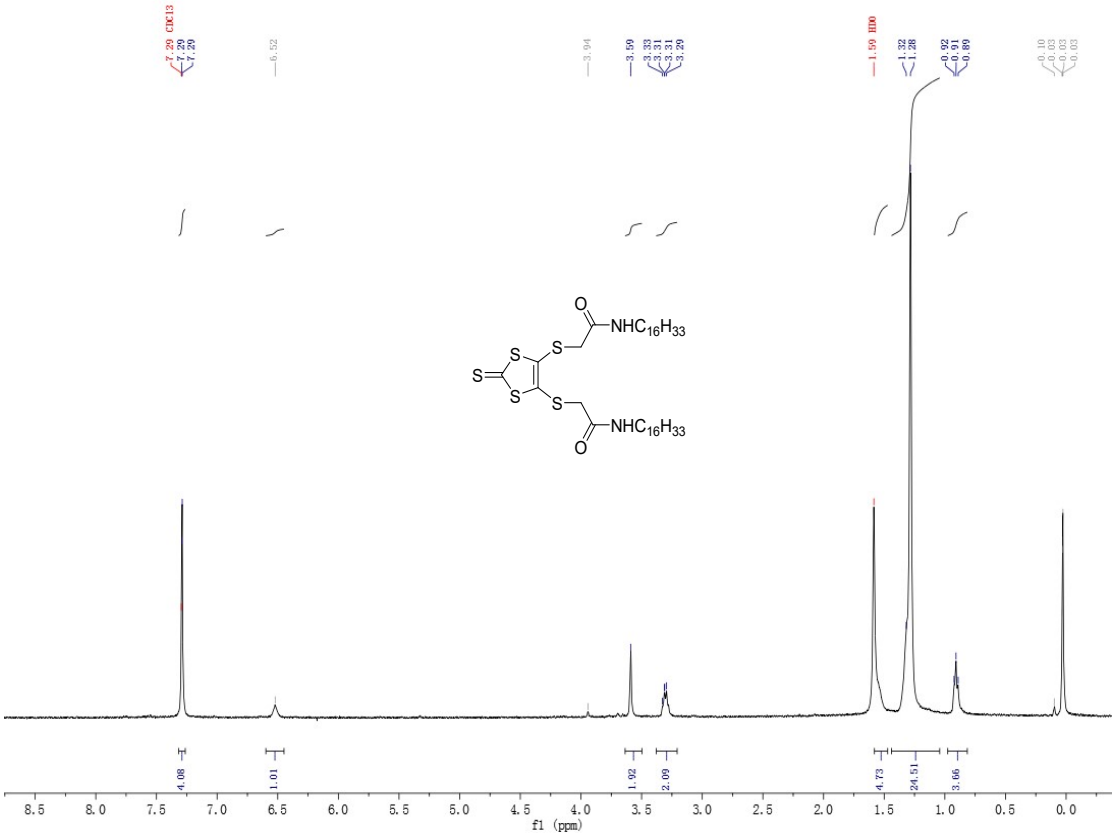

Fig. S6 ^{1}H NMR of derivative **2b**

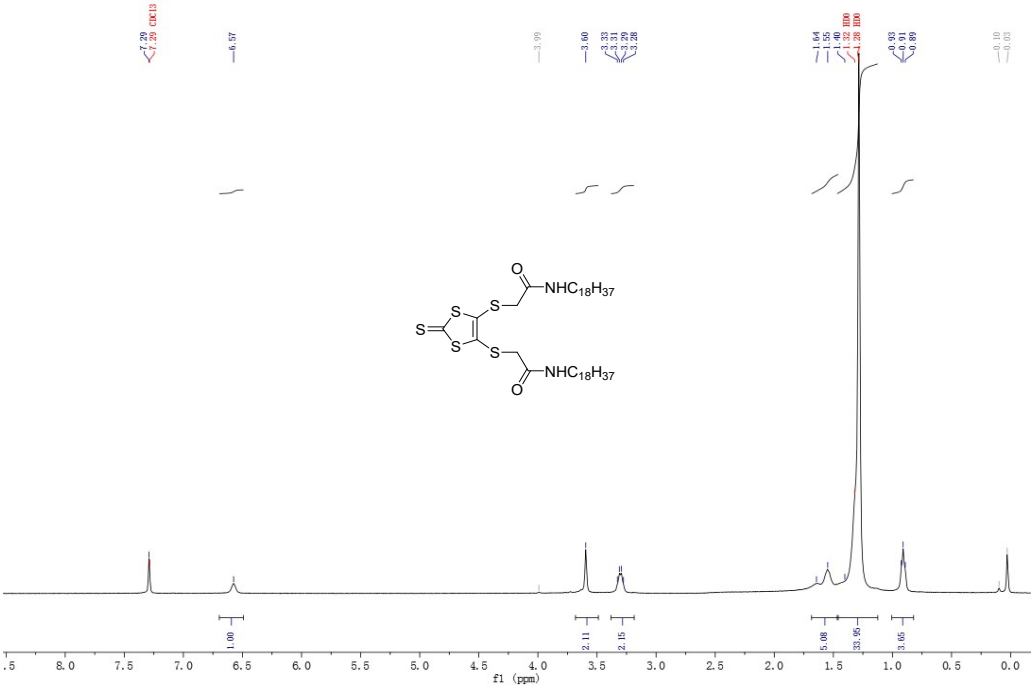

Fig. S7 ^{1}H NMR of the derivative **2c**

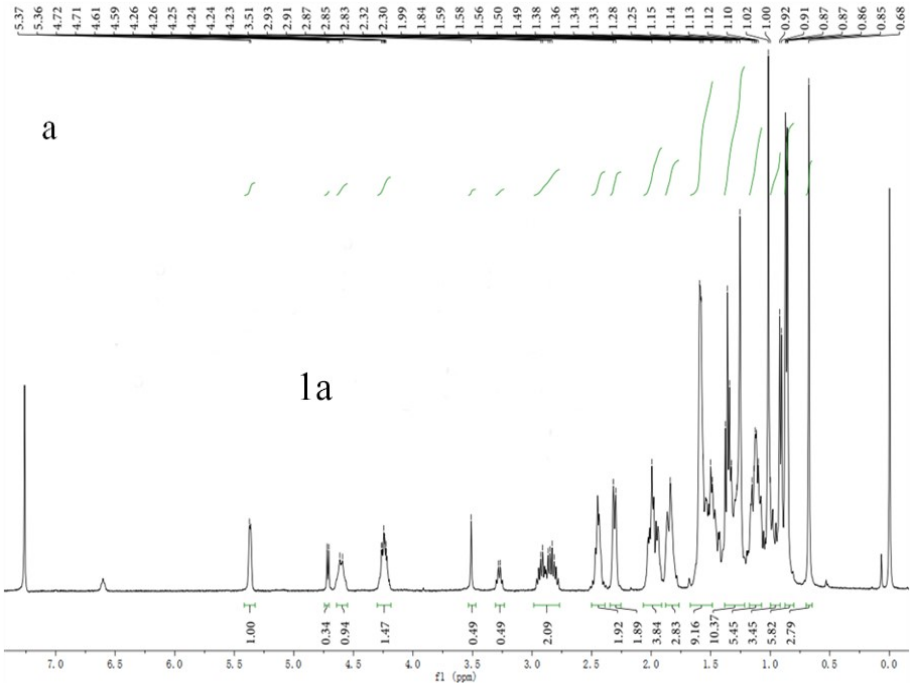
a
1a
f1 (ppm)

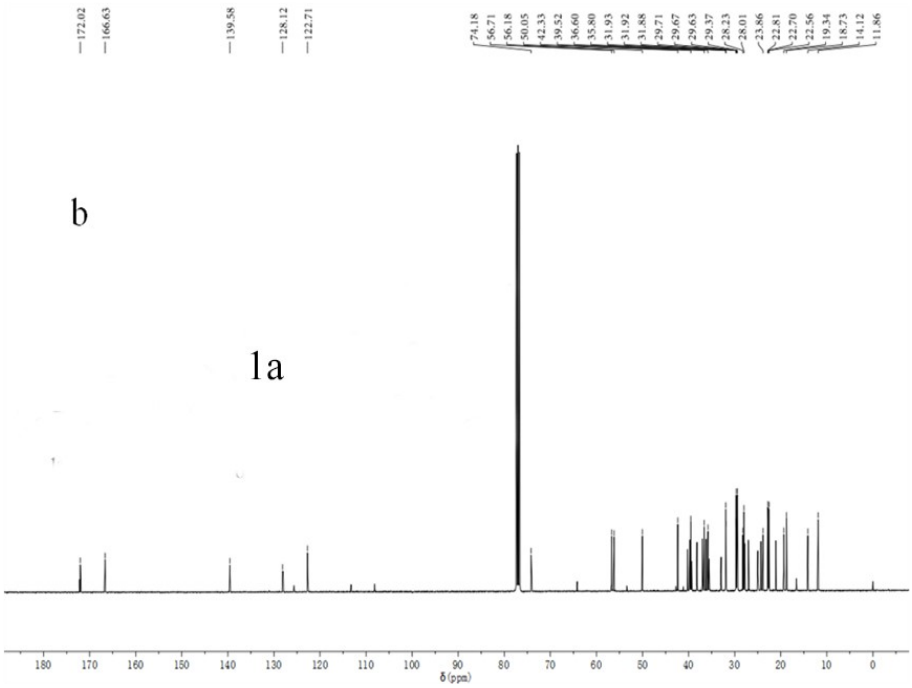
b
1a
δ (ppm)

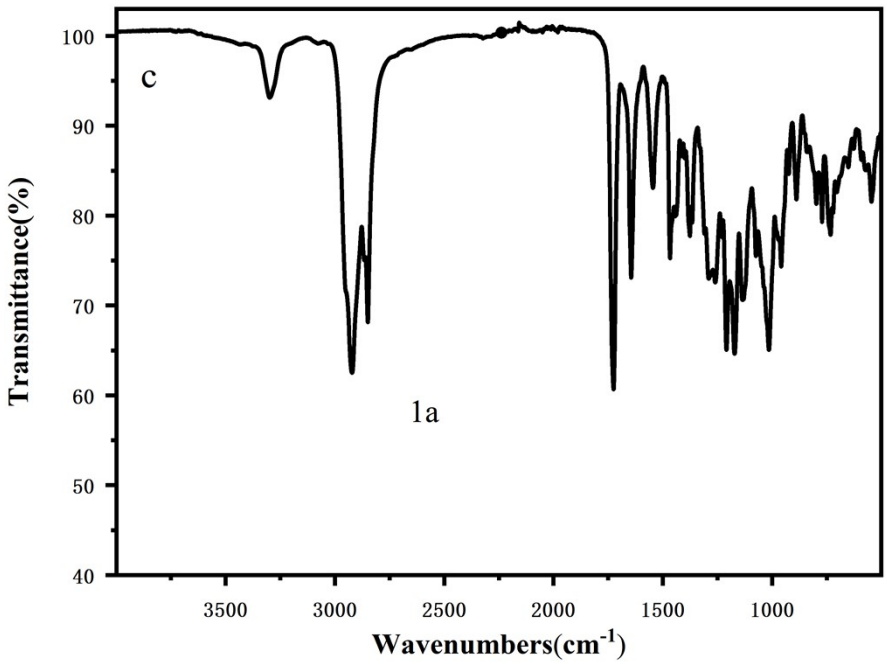

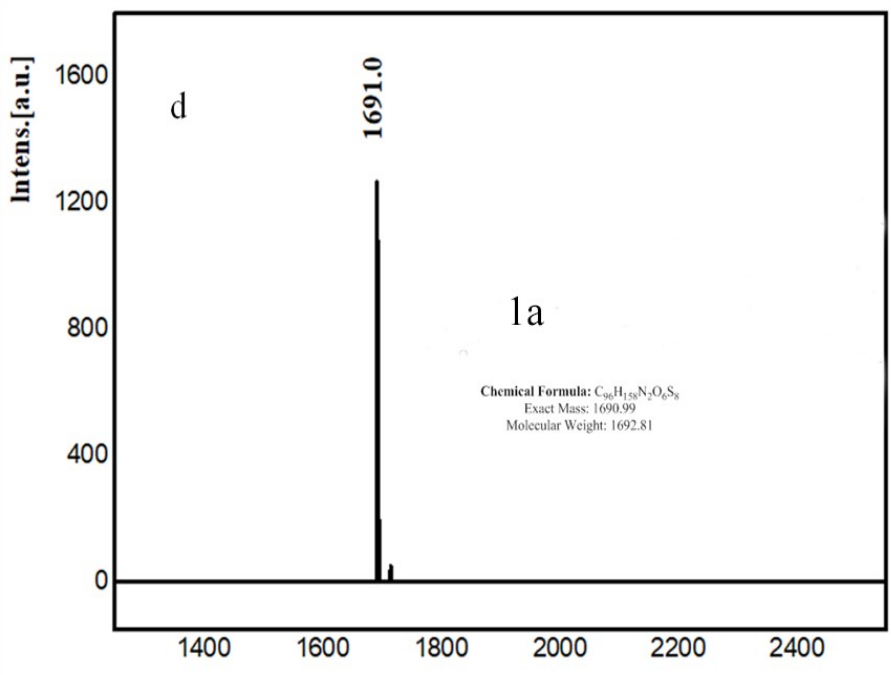

Fig. S8 (a) ^{1}H NMR of the target compound **1a**

(b) ^{13}C NMR of the target compound **1a**

(c) FT-IR of the target compound **1a**

(b) MALDI-TOF-MS of the target compound **1a**

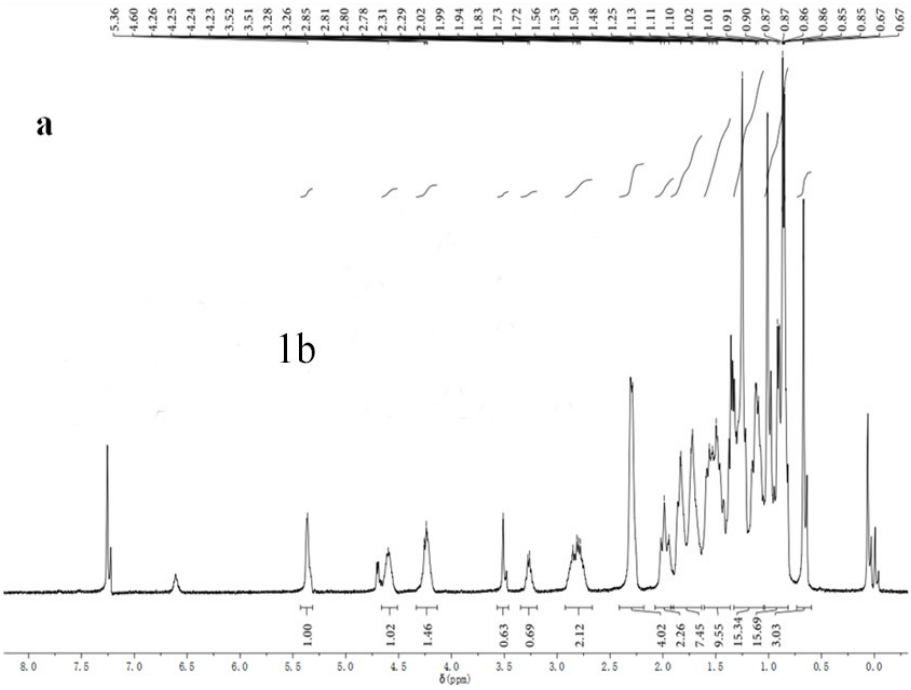
a
1b
5.36
4.60
4.26
4.25
4.24
4.23
3.52
3.51
3.28
3.26
2.85
2.81
2.80
2.78
2.31
2.29
2.02
1.99
1.94
1.83
1.73
1.72
1.56
1.53
1.50
1.48
1.25
1.13
1.11
1.10
1.02
1.01
0.91
0.90
0.87
0.86
0.86
0.85
0.85
0.67
0.67
1.00
1.02
1.46
0.63
0.69
2.12
4.02
2.26
7.45
9.55
15.34
15.69
3.03
8.0
7.5
7.0
6.5
6.0
5.5
5.0
4.5
4.0
3.5
3.0
2.5
2.0
1.5
1.0
0.5
0.0
δ(ppm)

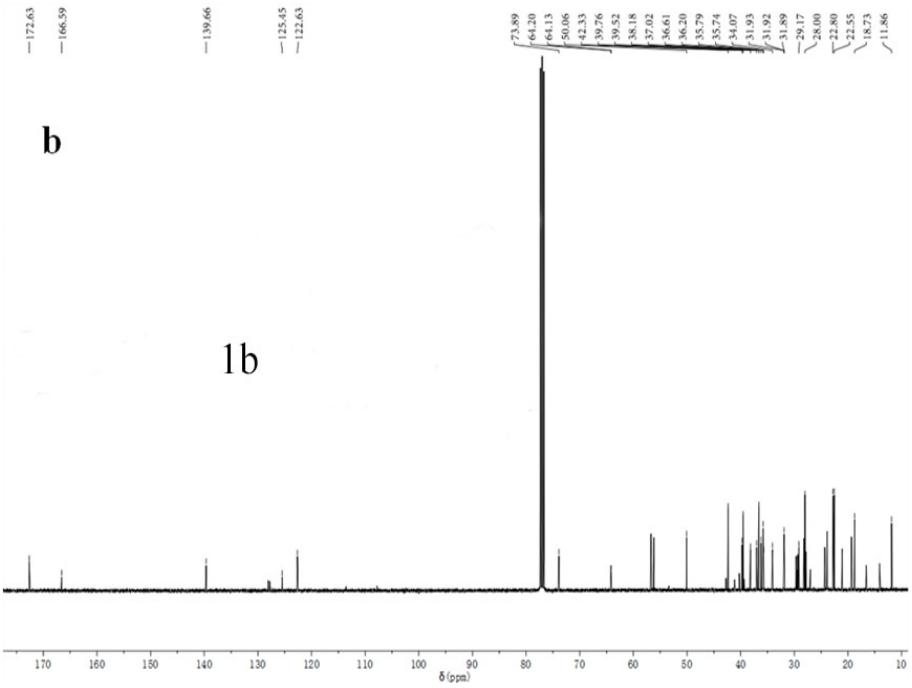
b
1b
172.63
166.59
139.66
125.45
122.63
73.89
64.20
64.13
50.06
42.33
39.76
39.52
38.18
37.02
36.61
36.20
35.79
35.74
34.07
31.93
31.92
31.89
29.17
28.00
22.80
22.55
18.73
11.86
170
160
150
140
130
120
110
100
90
80
70
60
50
40
30
20
10
δ(ppm)

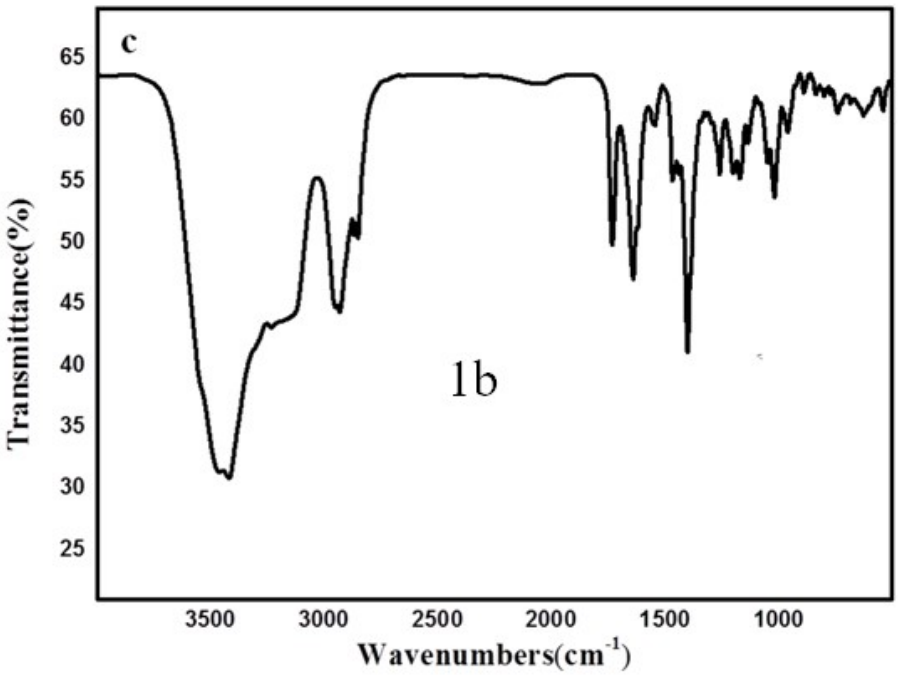

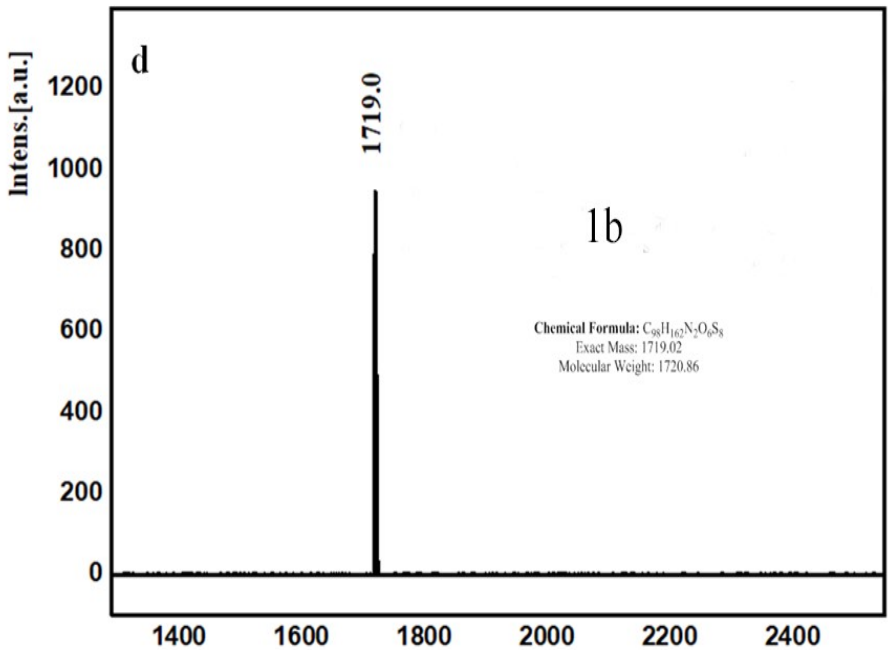

Fig. S9 (a) ^{1}H NMR of the target compound **1b**

(b) ^{13}C NMR of the target compound **1b**

(c) FT-IR of the target compound **1b**

(b) MALDI-TOF-MS of the target compound **1b**

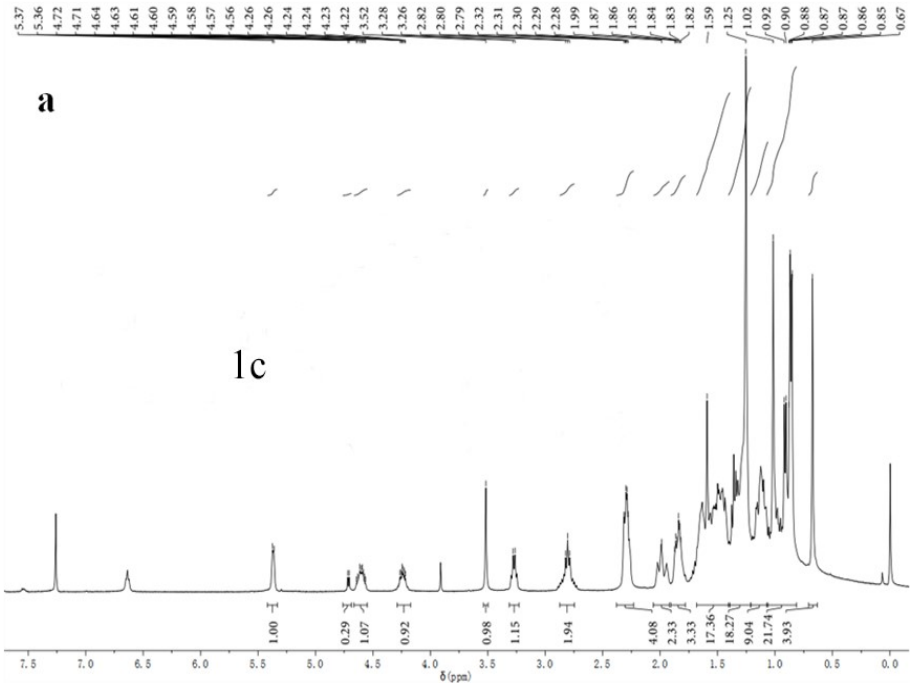
a
1c
δ(ppm)

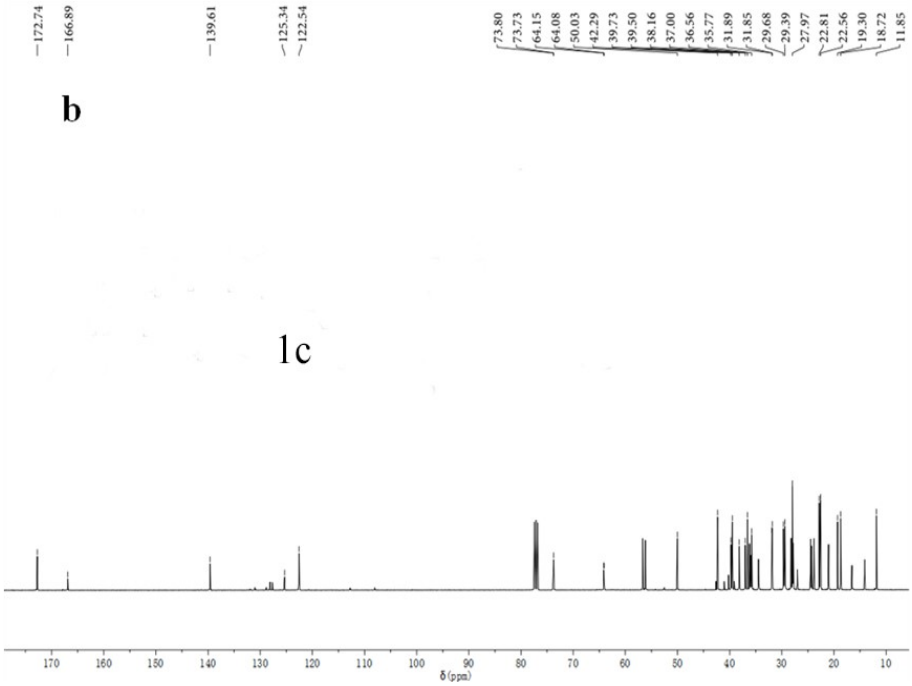
b
1c
δ(ppm)

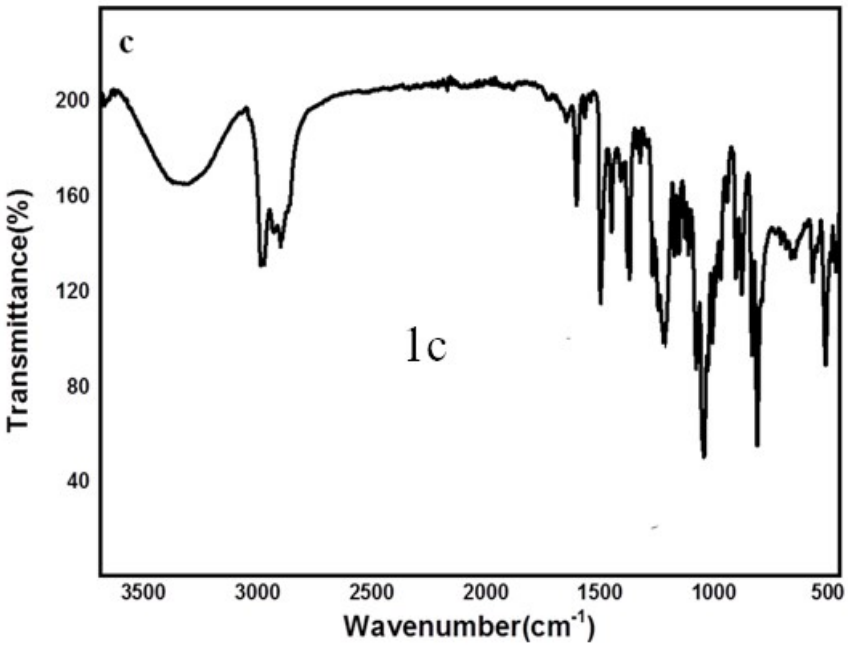

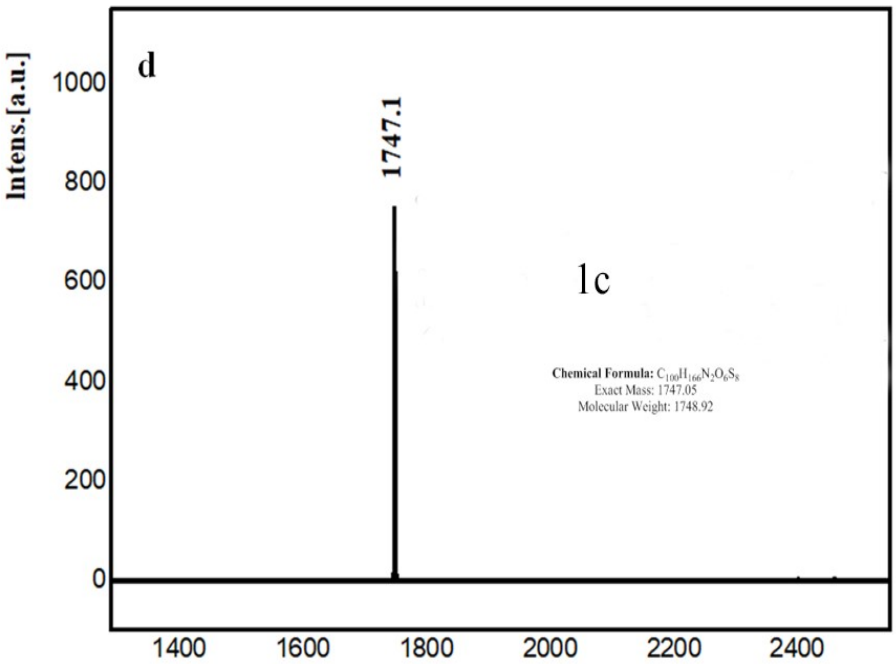

Fig. S10 (a) ^{1}H NMR of the target compound **1c**

(b) ^{13}C NMR of the target compound **1c**

(c) FT-IR of the target compound **1c**

(b) MALDI-TOF-MS of the target compound **1c**

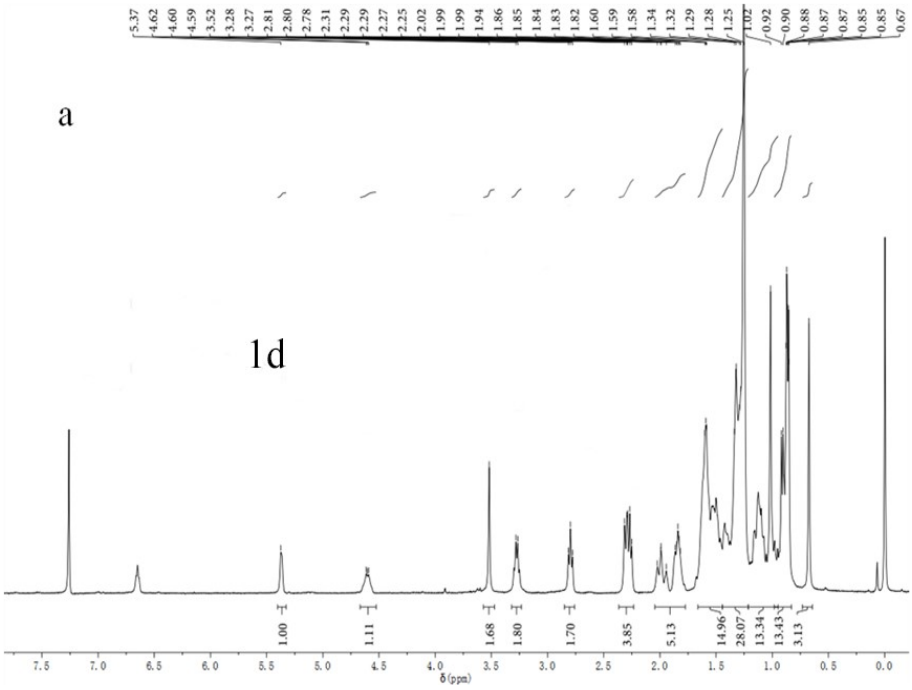
a
1d
δ(ppm)

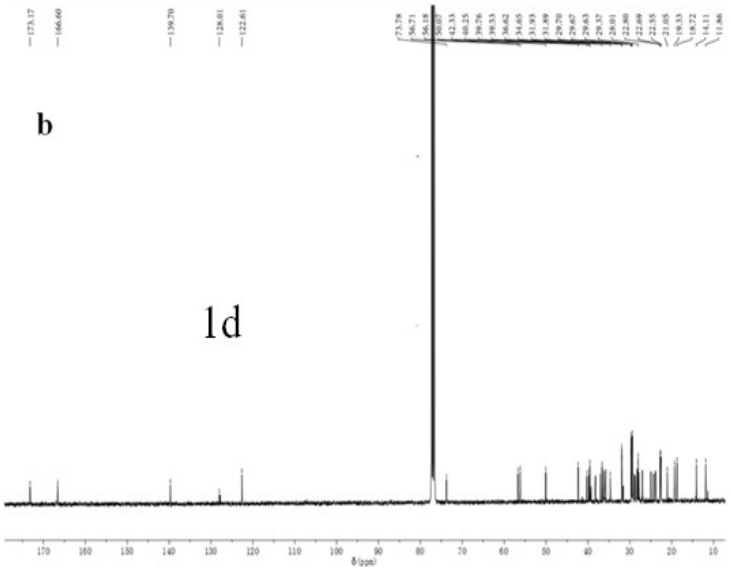
b
1d
δ(ppm)

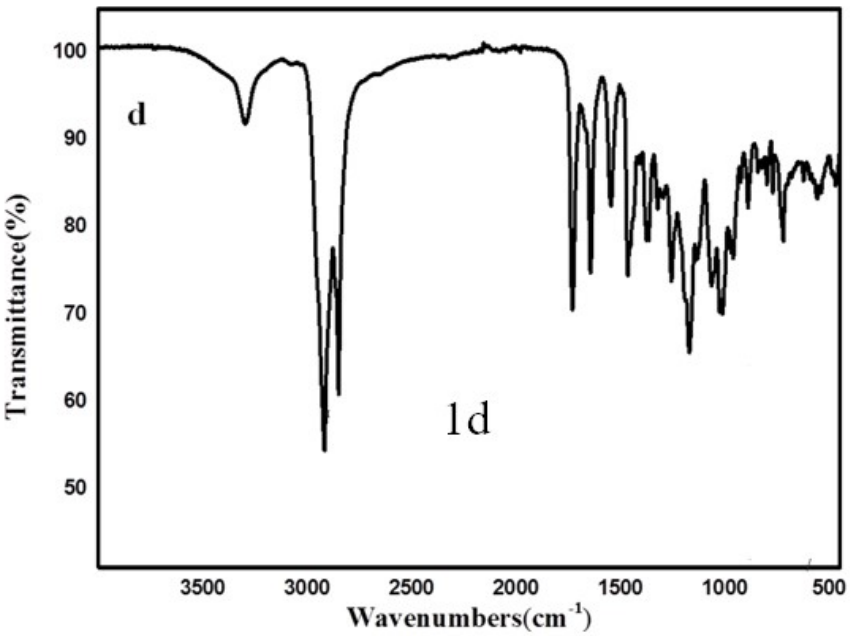

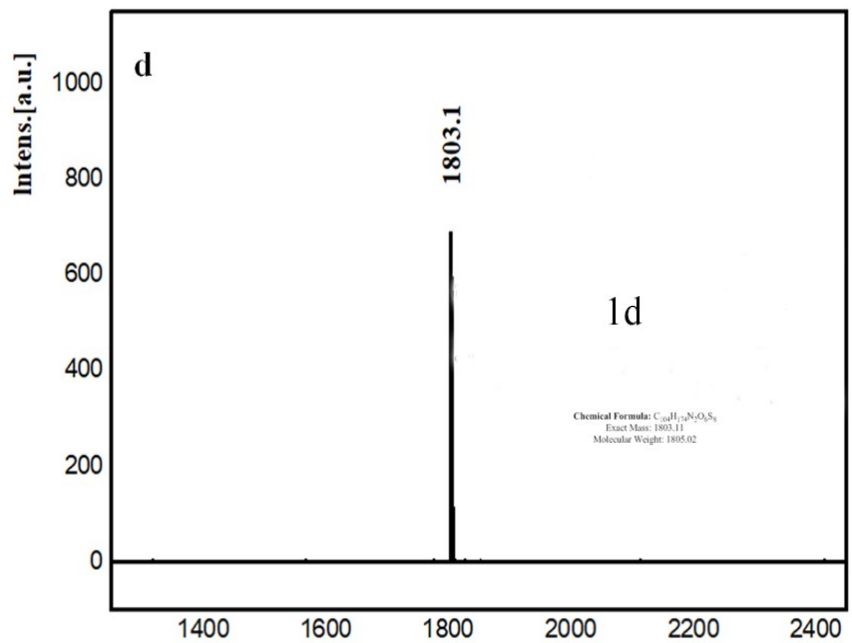

Fig. S11 (a) ^{1}H NMR of the target compound **1d**

(b) ^{13}C NMR of the target compound **1d**

(c) FT-IR of the target compound **1d**

(b) MALDI-TOF-MS of the target compound **1d**

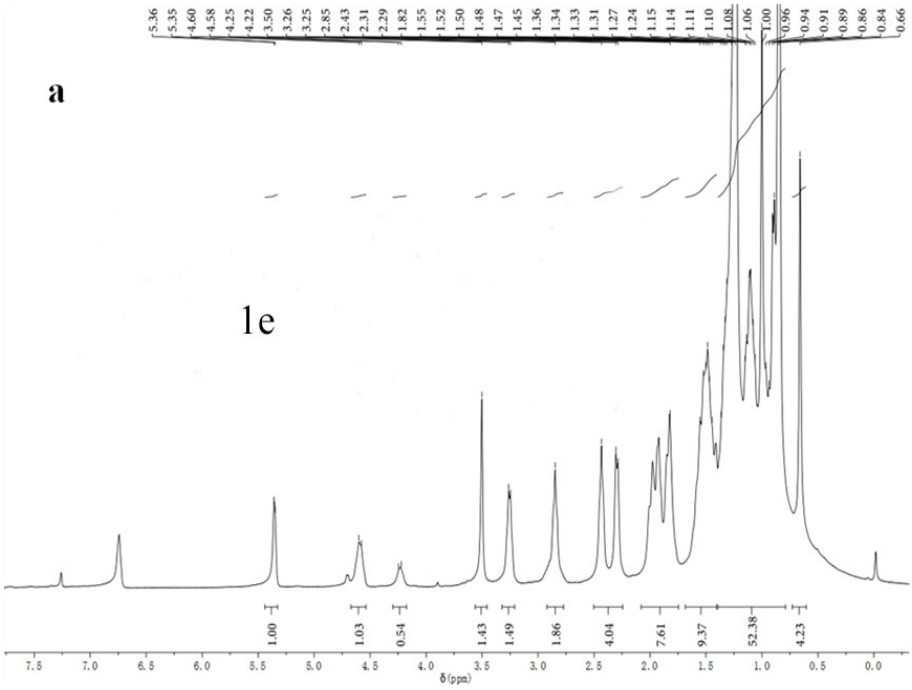
a
1e
5.36
5.35
4.60
4.58
4.25
4.22
3.50
3.26
3.25
2.85
2.43
2.31
2.29
1.82
1.55
1.52
1.50
1.48
1.47
1.45
1.36
1.34
1.33
1.31
1.27
1.24
1.15
1.14
1.11
1.10
1.08
1.06
1.00
0.96
0.94
0.91
0.89
0.86
0.84
0.66
1.00
1.03
0.54
1.43
1.49
1.86
4.04
7.61
9.37
52.38
4.23
7.5
7.0
6.5
6.0
5.5
5.0
4.5
4.0
3.5
3.0
2.5
2.0
1.5
1.0
0.5
0.0
δ(ppm)

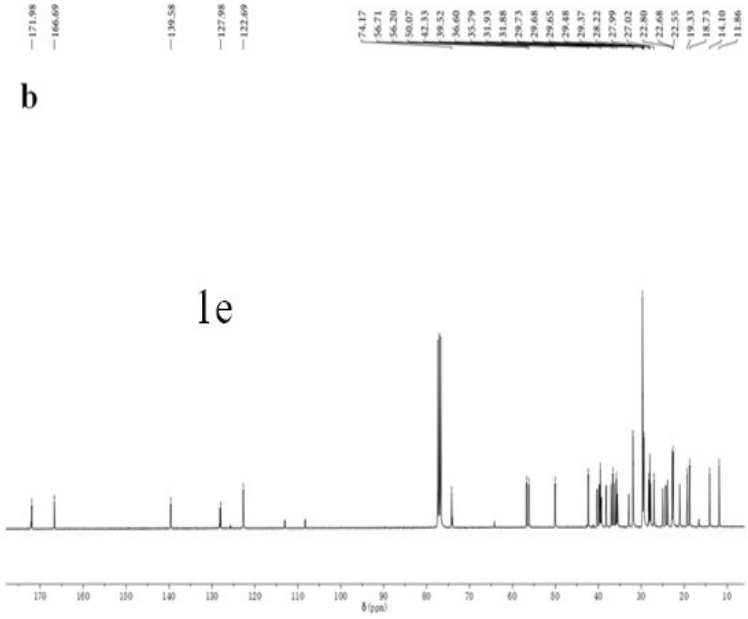
171.98
166.69
139.58
127.98
122.69
74.17
56.71
56.20
50.07
42.33
39.52
36.60
35.79
31.93
31.88
29.73
29.68
29.65
29.48
29.37
28.22
27.99
27.02
22.80
22.68
22.55
19.33
18.73
14.10
11.86
b
1e
170
160
150
140
130
120
110
100
90
80
70
60
50
40
30
20
10
δ(ppm)

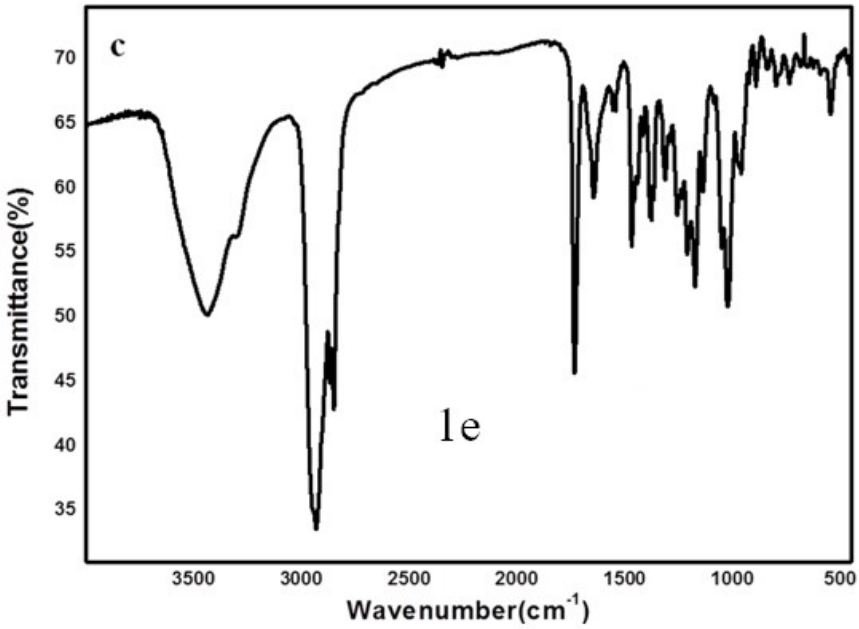

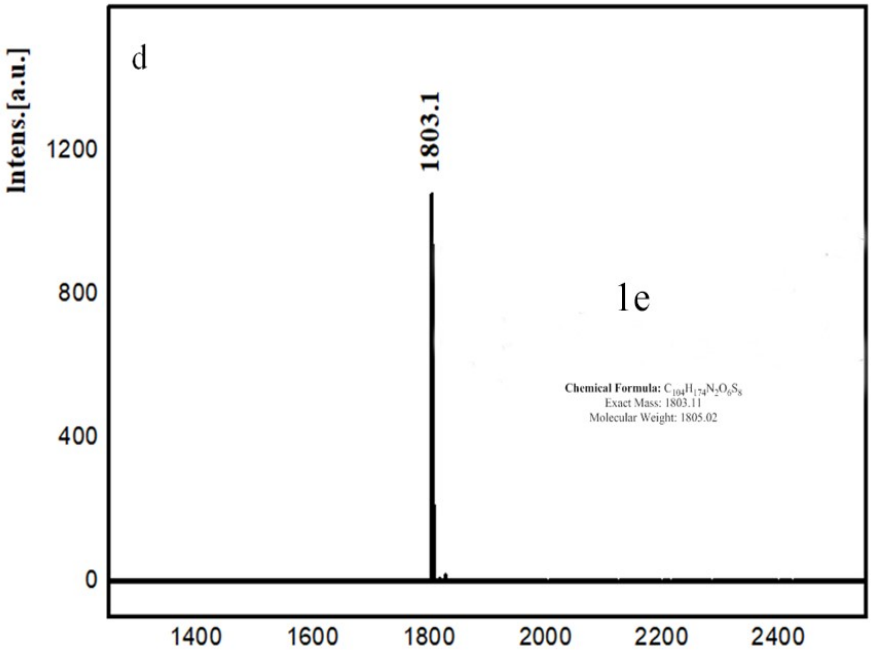

Fig. S12 (a) ^{1}H NMR of the target compound **1e**

(b) ^{13}C NMR of the target compound **1e**

(c) FT-IR of the target compound **1e**

(b) MALDI-TOF-MS of the target compound **1e**

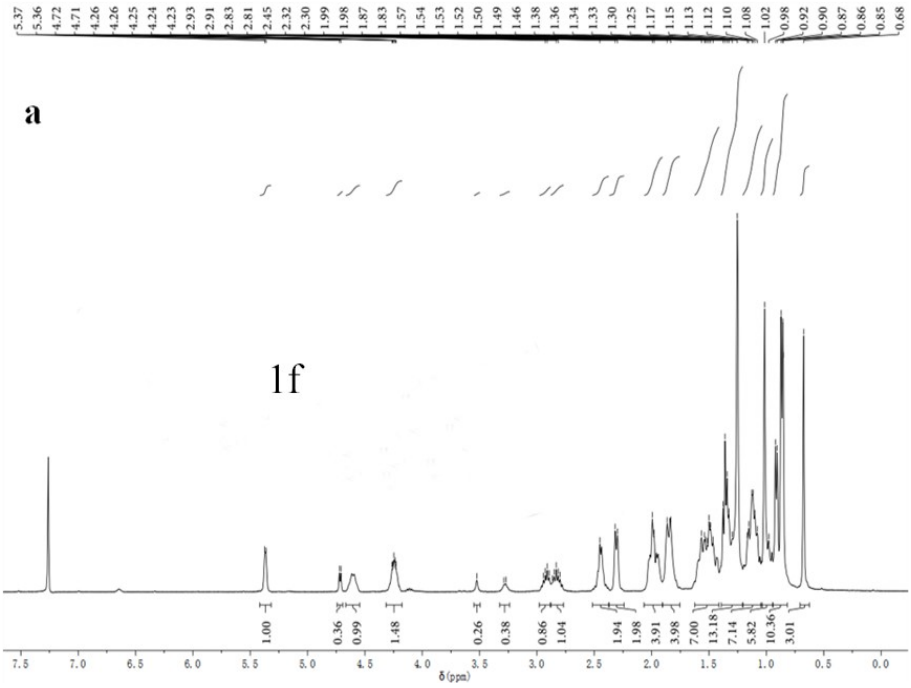
a
1f
δ(ppm)

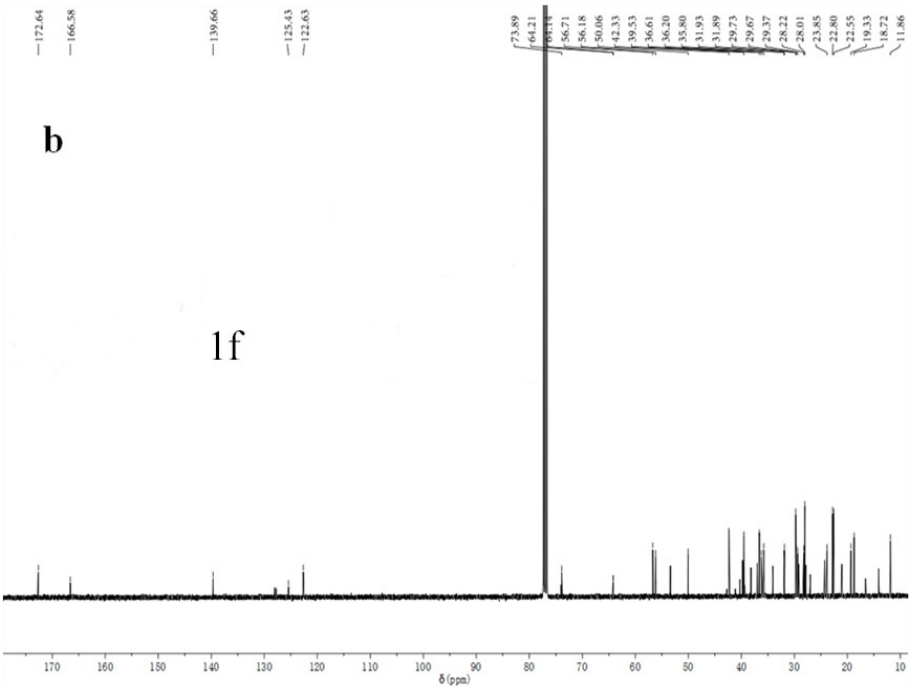
b
1f
δ(ppm)

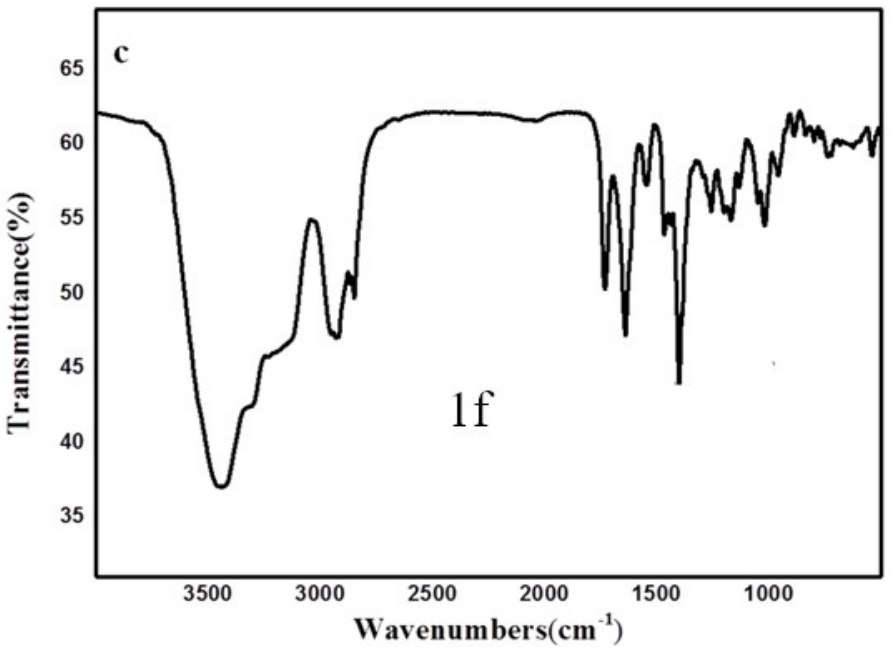

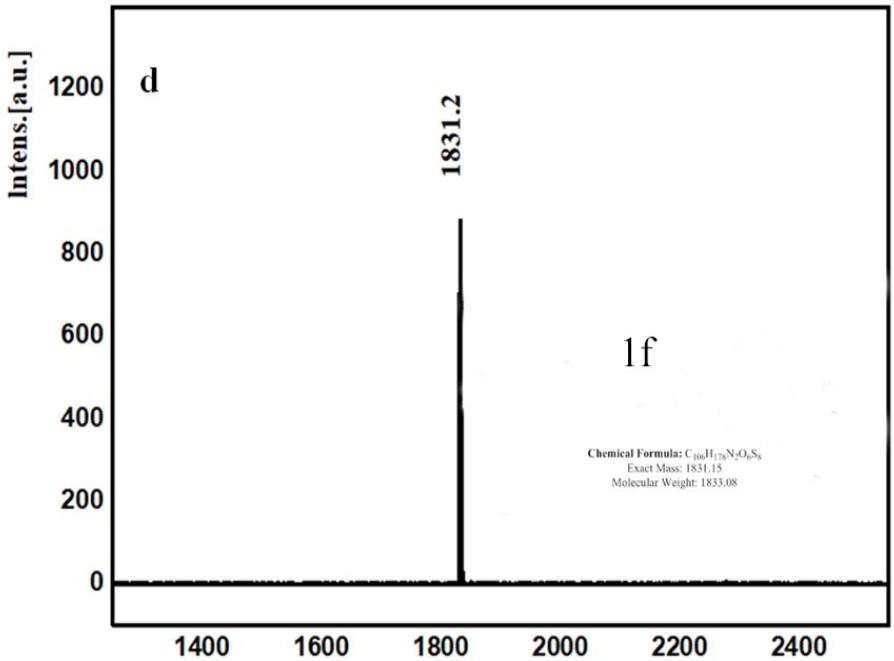

Fig. S13 (a) ^{1}H NMR of the target compound **1f**

(b) ^{13}C NMR of the target compound **1f**

(c) FT-IR of the target compound **1f**

(b) MALDI-TOF-MS of the target compound **1f**

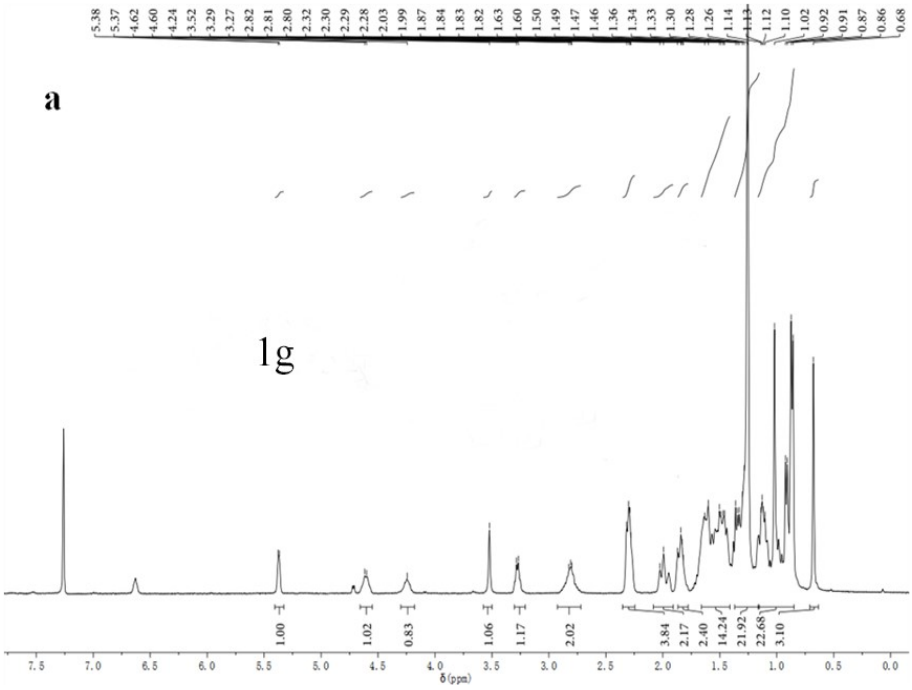
a
1g
5.38
5.37
4.62
4.60
4.24
3.52
3.29
3.27
2.82
2.81
2.80
2.32
2.30
2.29
2.28
2.03
1.99
1.87
1.84
1.83
1.82
1.63
1.60
1.50
1.49
1.47
1.46
1.36
1.34
1.33
1.30
1.28
1.26
1.14
1.13
1.12
1.10
1.02
0.92
0.91
0.87
0.86
0.68
1.00
1.02
0.83
1.06
1.17
2.02
3.84
2.17
2.40
14.24
21.92
22.68
3.10
7.5
7.0
6.5
6.0
5.5
5.0
4.5
4.0
3.5
3.0
2.5
2.0
1.5
1.0
0.5
0.0
δ(ppm)

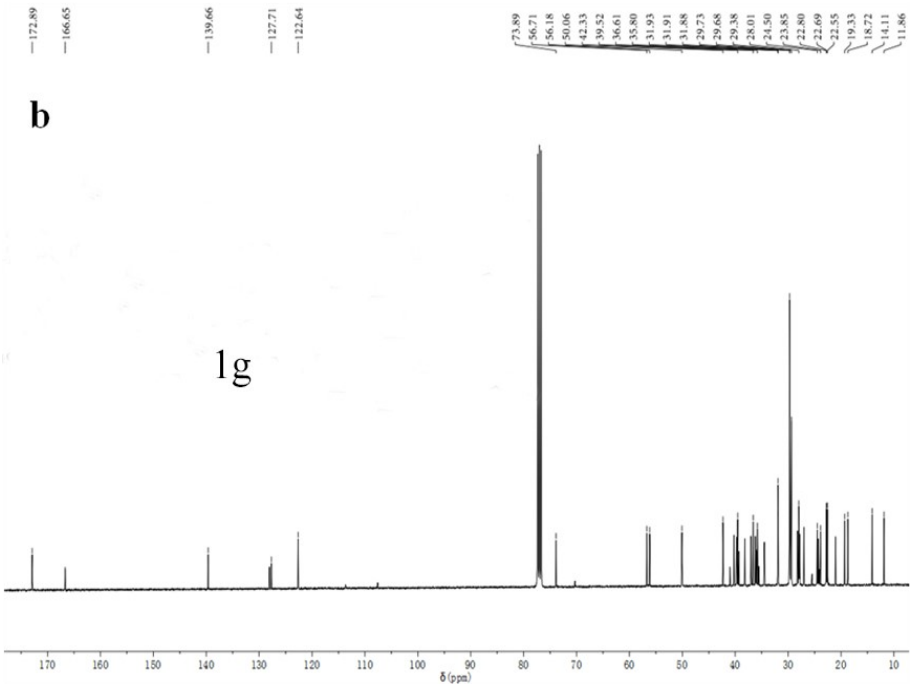
b
1g
172.89
166.65
139.66
127.71
122.64
73.89
56.71
56.18
50.06
42.33
39.52
36.61
35.80
31.93
31.91
31.88
29.73
29.68
29.38
28.01
24.50
23.85
22.80
22.69
22.55
19.33
18.72
14.11
11.86
170
160
150
140
130
120
110
100
90
80
70
60
50
40
30
20
10
δ(ppm)

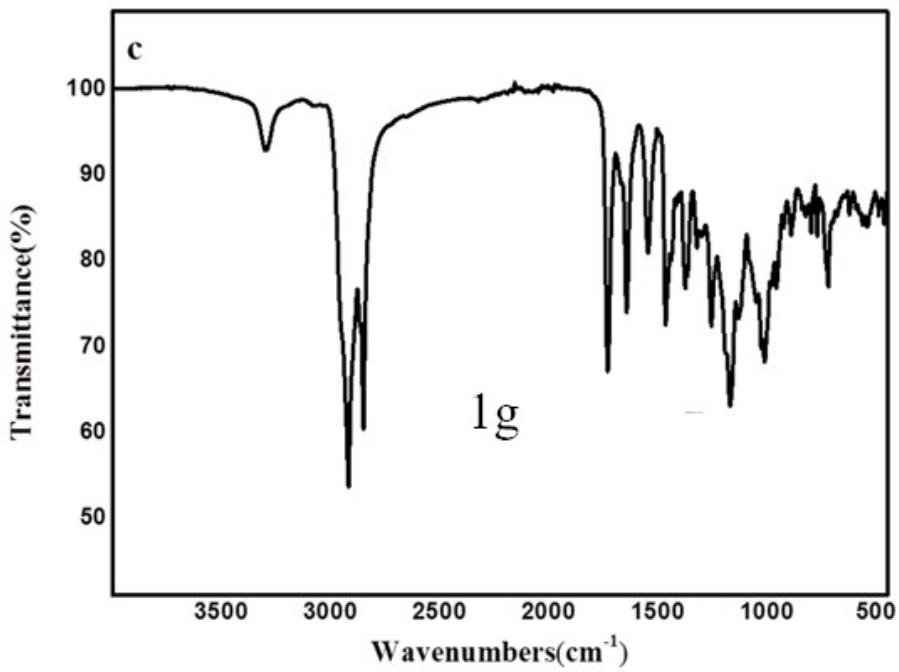

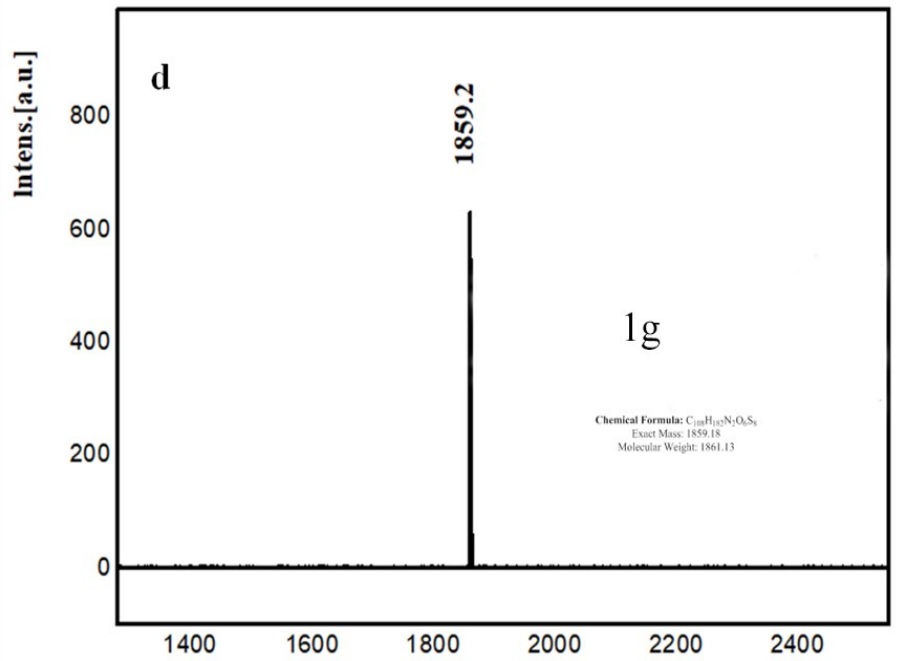

Fig. S14 (a) ^{1}H NMR of the target compound **1g**

(b) ^{13}C NMR of the target compound **1g**

(c) FT-IR of the target compound **1g**

(b) MALDI-TOF-MS of the target compound **1g**

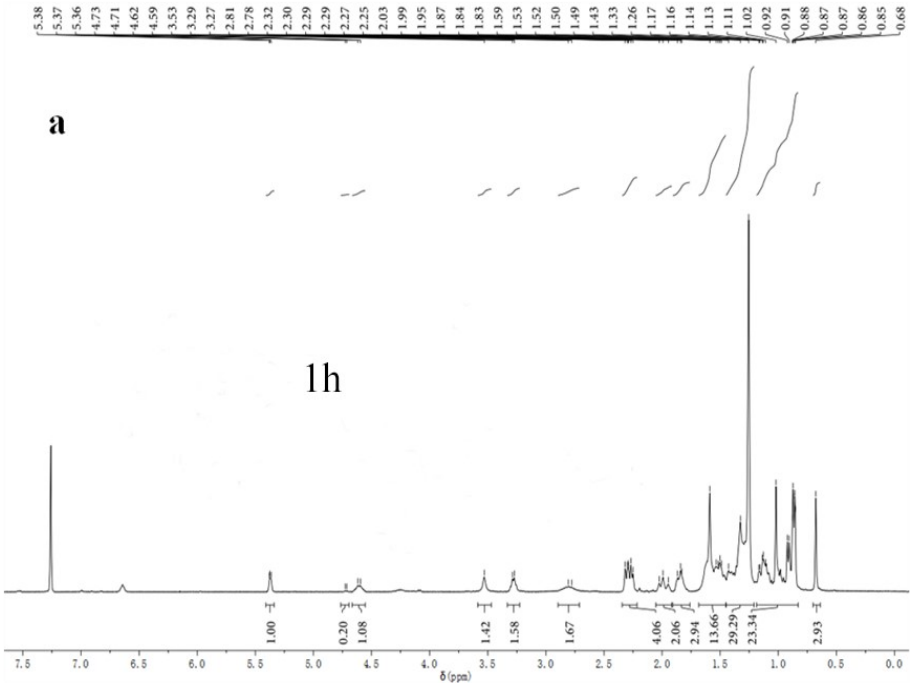
a
1h
δ(ppm)

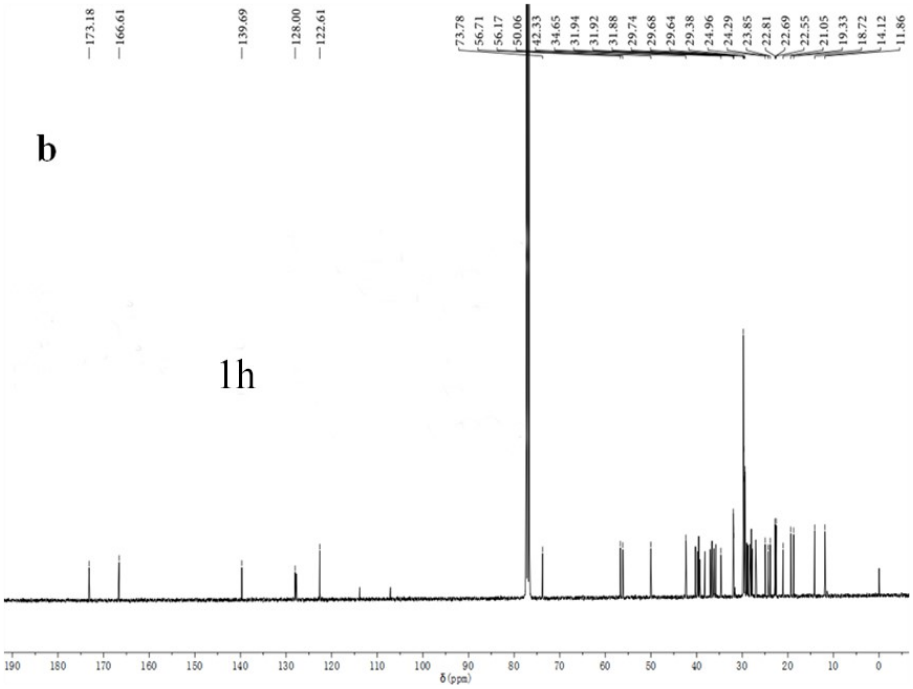
b
1h
δ(ppm)

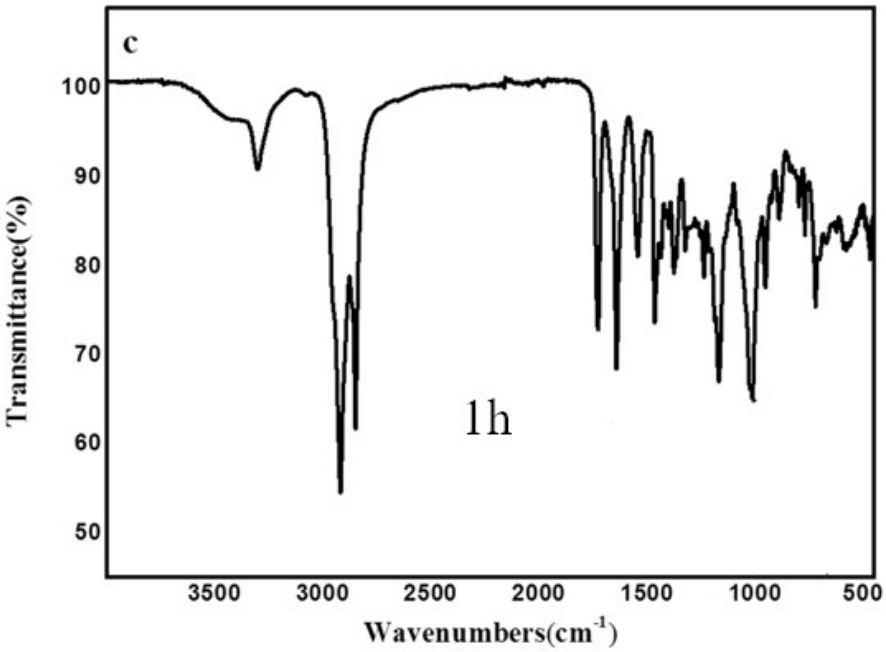

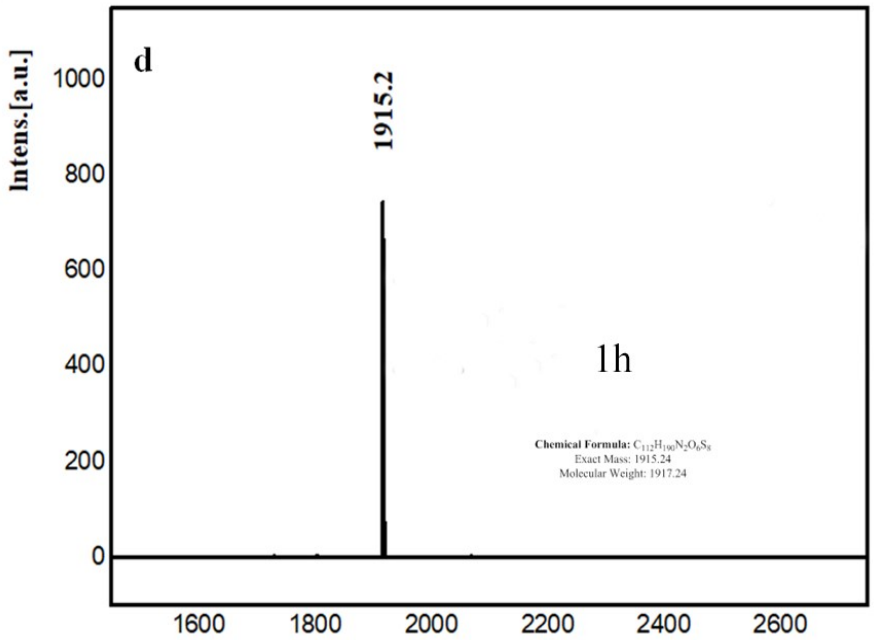

Fig. S15 (a) ^{1}H NMR of the target compound **1h**

(b) ^{13}C NMR of the target compound **1h**

(c) FT-IR of the target compound **1h**

(b) MALDI-TOF-MS of the target compound **1h**

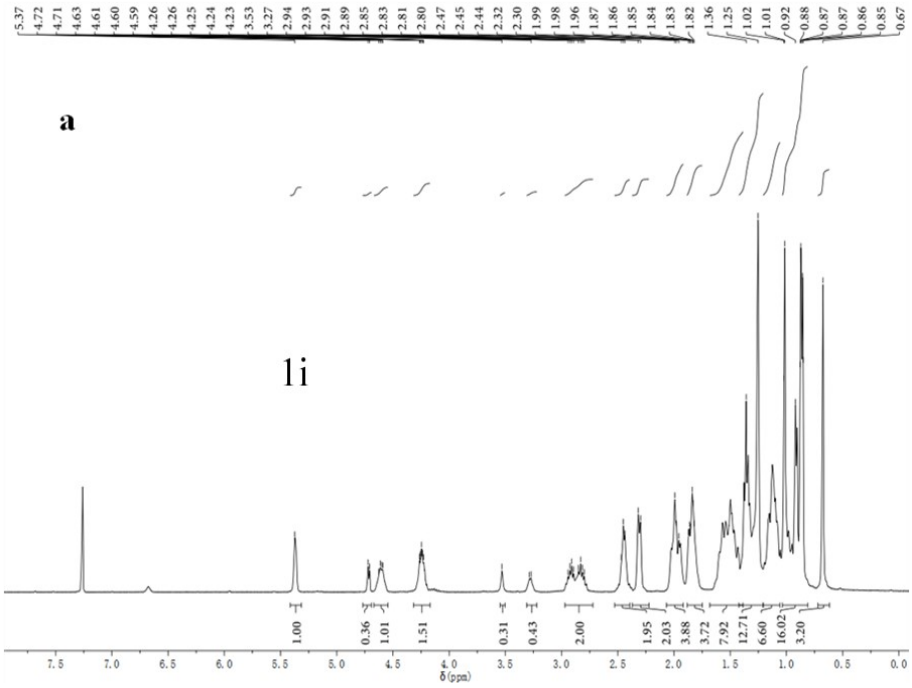
a
1i
δ(ppm)

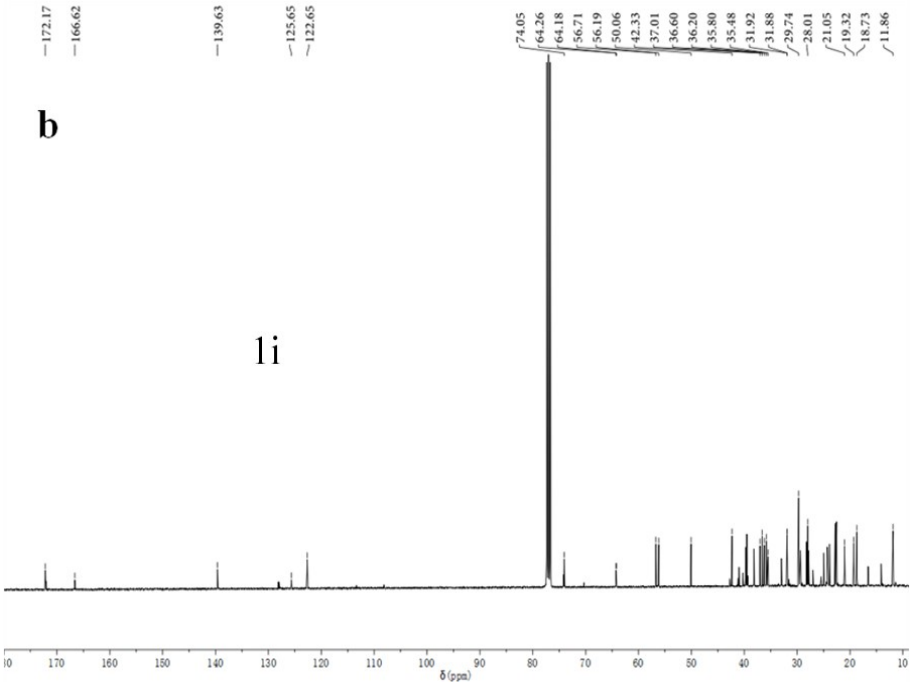
b
1i
δ(ppm)

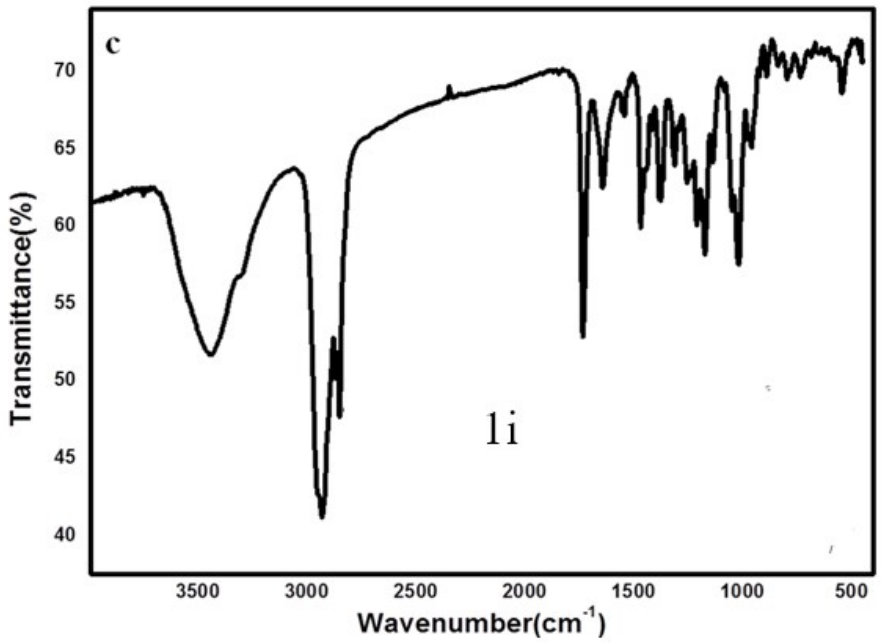

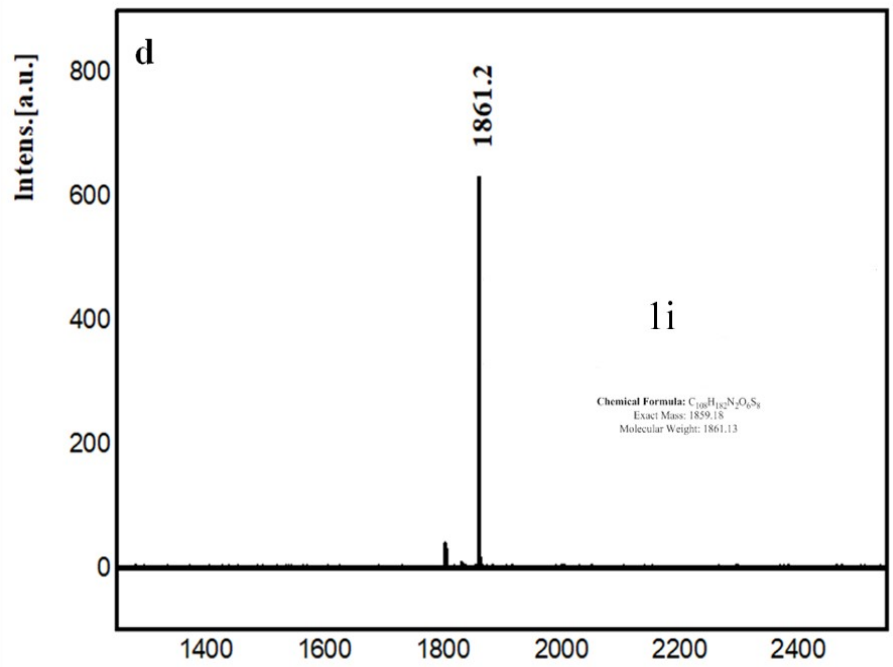

Fig. S16 (a) ^{1}H NMR of the target compound **1i**

(b) ^{13}C NMR of the target compound **1i**

(c) FT-IR of the target compound **1i**

(b) MALDI-TOF-MS of the target compound **1i**

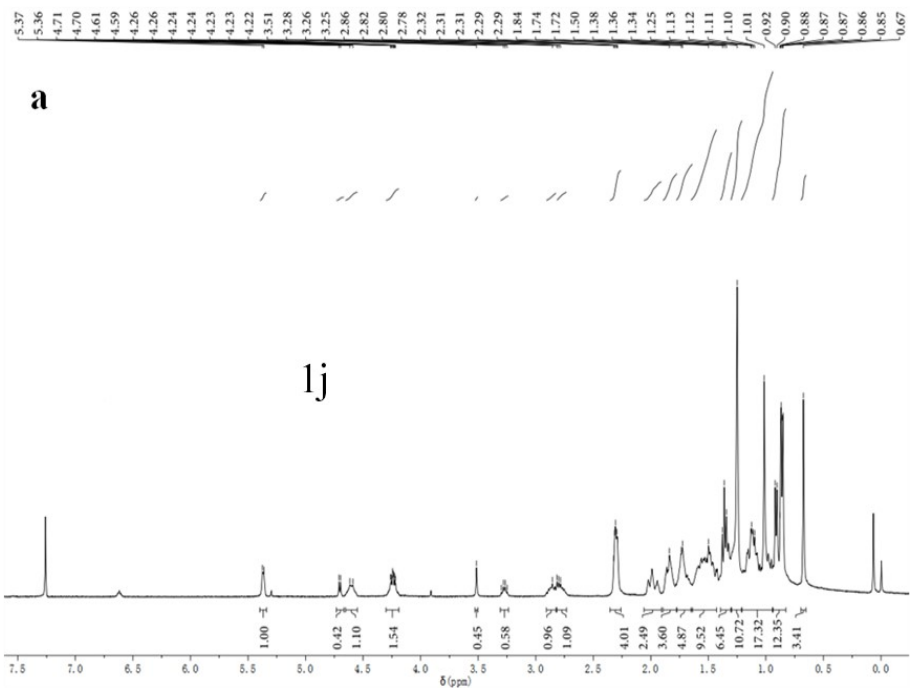
a
1j
δ(ppm)

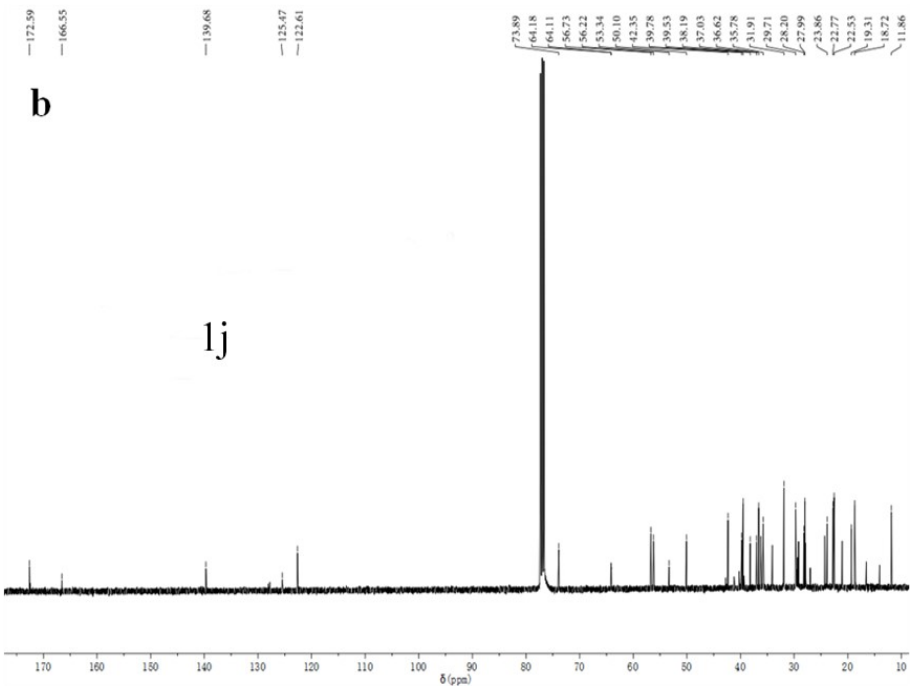
b
1j
δ(ppm)

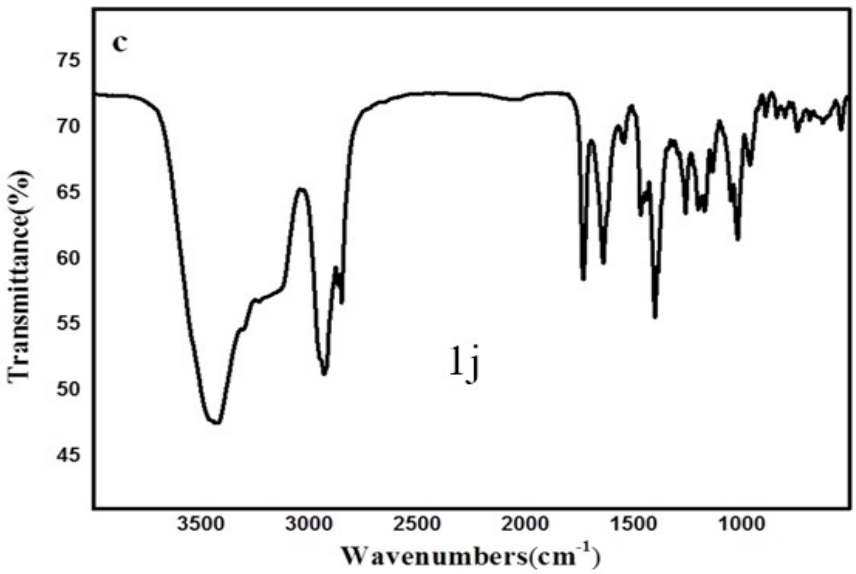

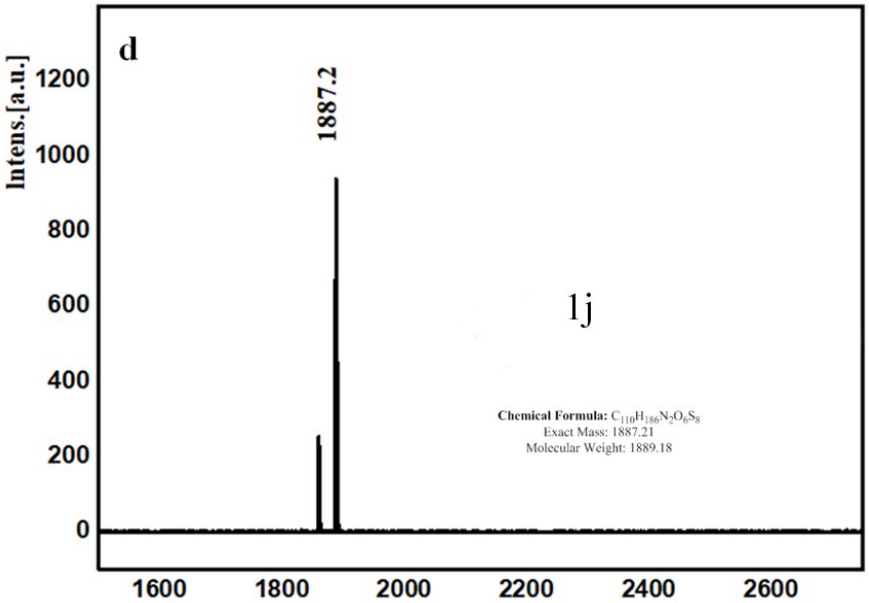

Fig. S17 (a) ^{1}H NMR of the target compound **1j**

(b) ^{13}C NMR of the target compound **1j**

(c) FT-IR of the target compound **1j**

(b) MALDI-TOF-MS of the target compound **1j**

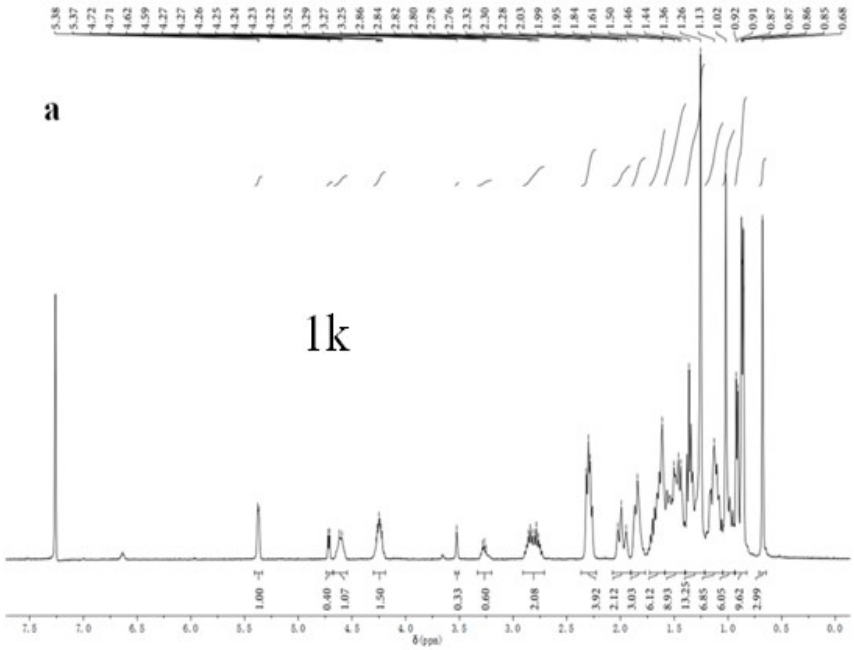
a
1k
δ (ppm)

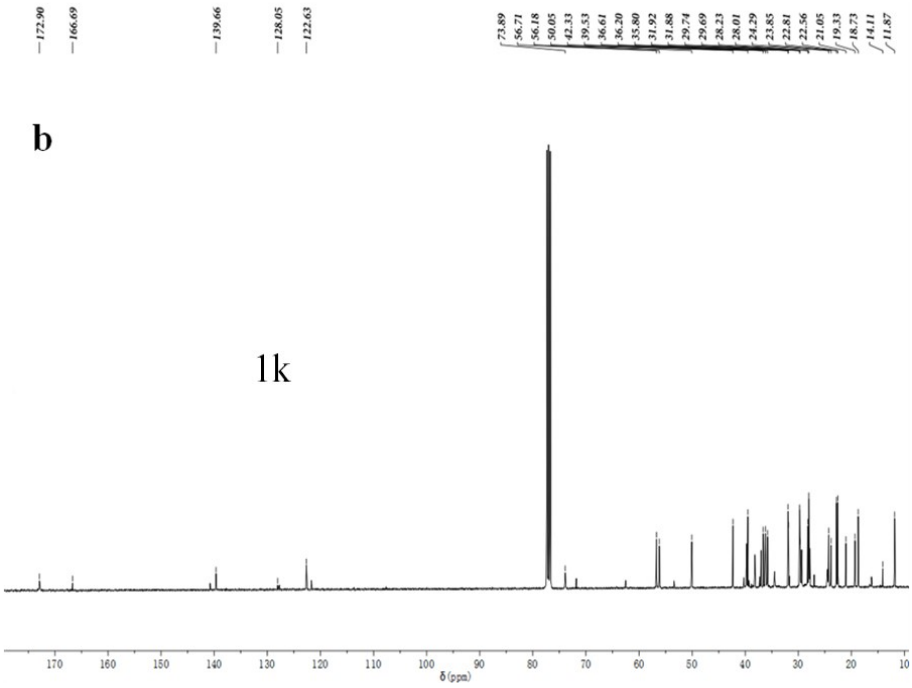
b
1k
δ (ppm)

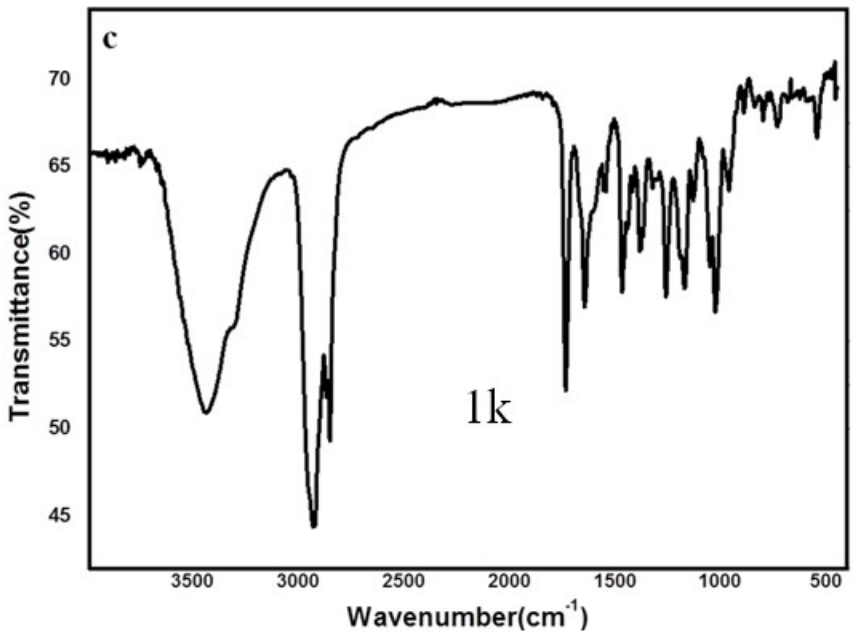

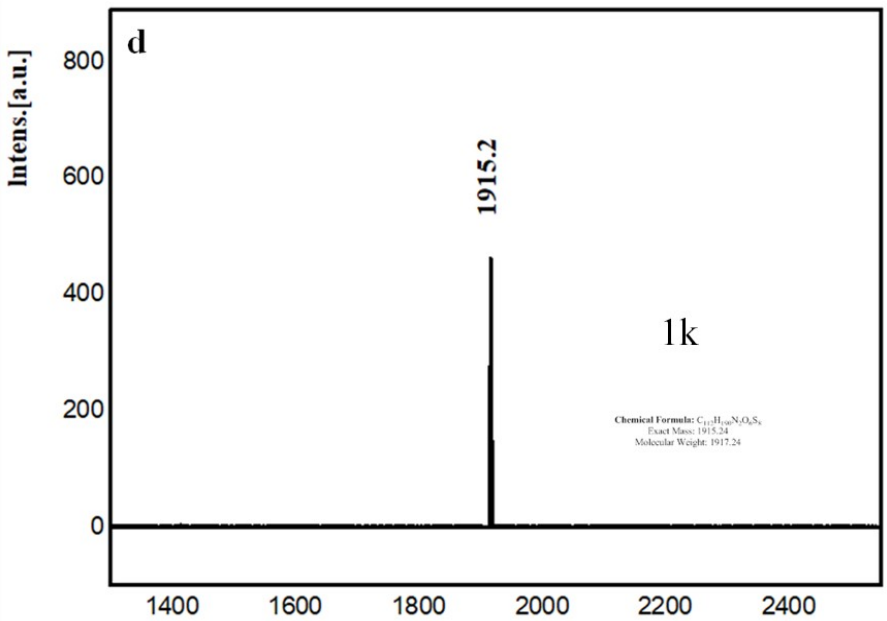

Fig. S18 (a) ^{1}H NMR of the target compound **1k**

(b) ^{13}C NMR of the target compound **1k**

(c) FT-IR of the target compound **1k**

(b) MALDI-TOF-MS of the target compound **1k**

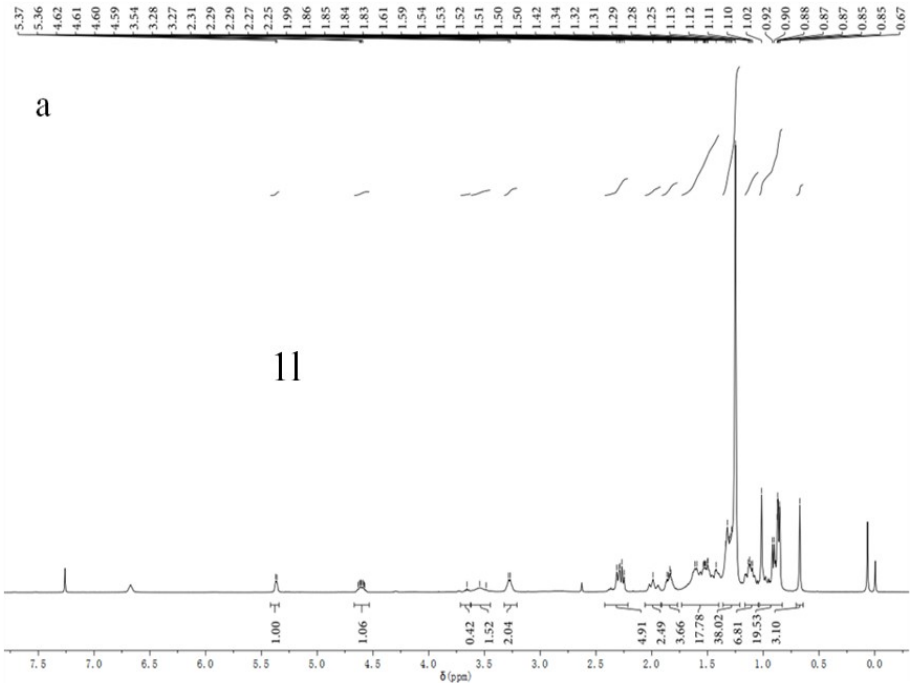
a
11
δ(ppm)

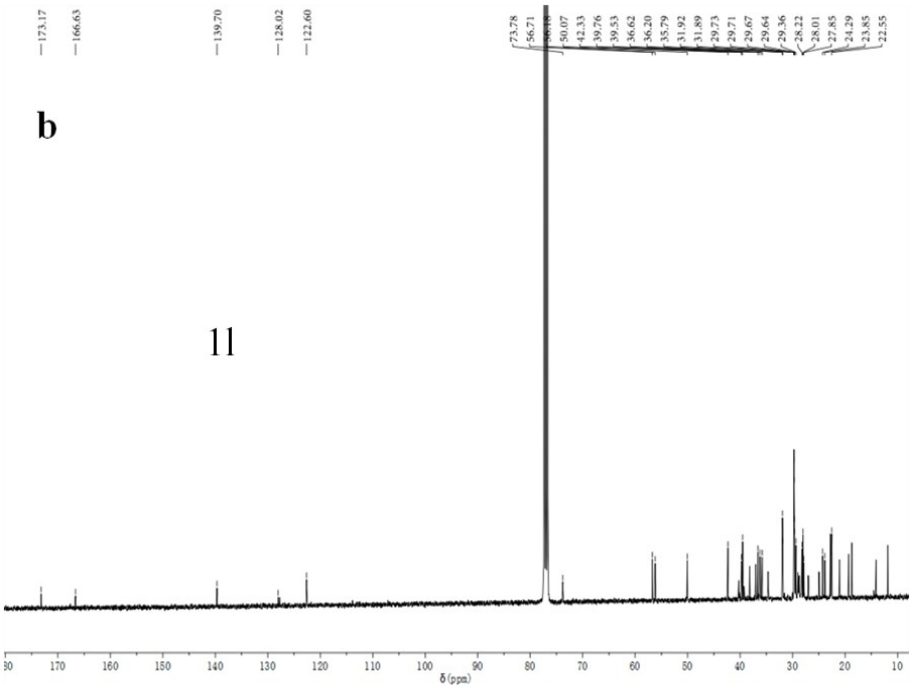
b
11
δ(ppm)

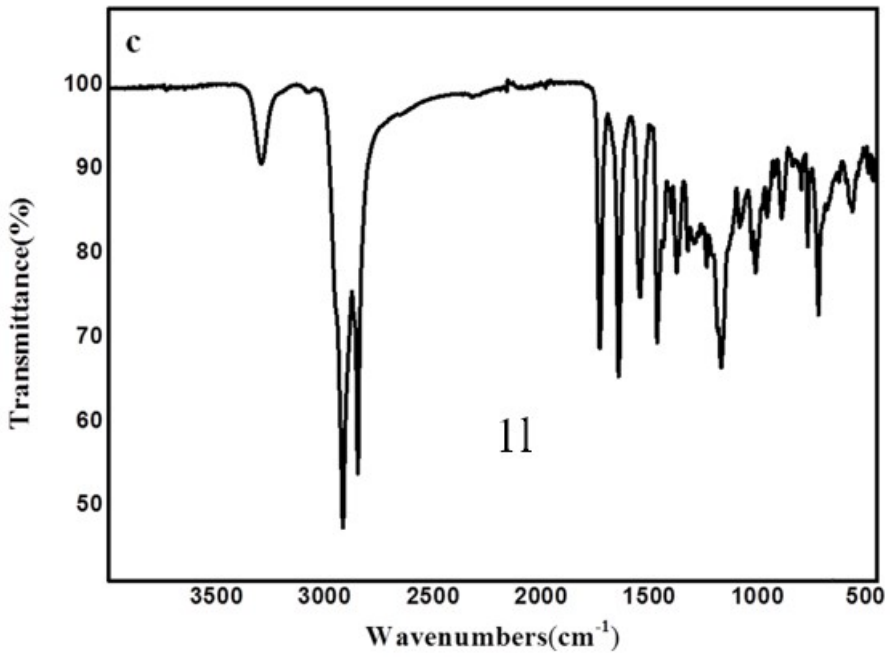

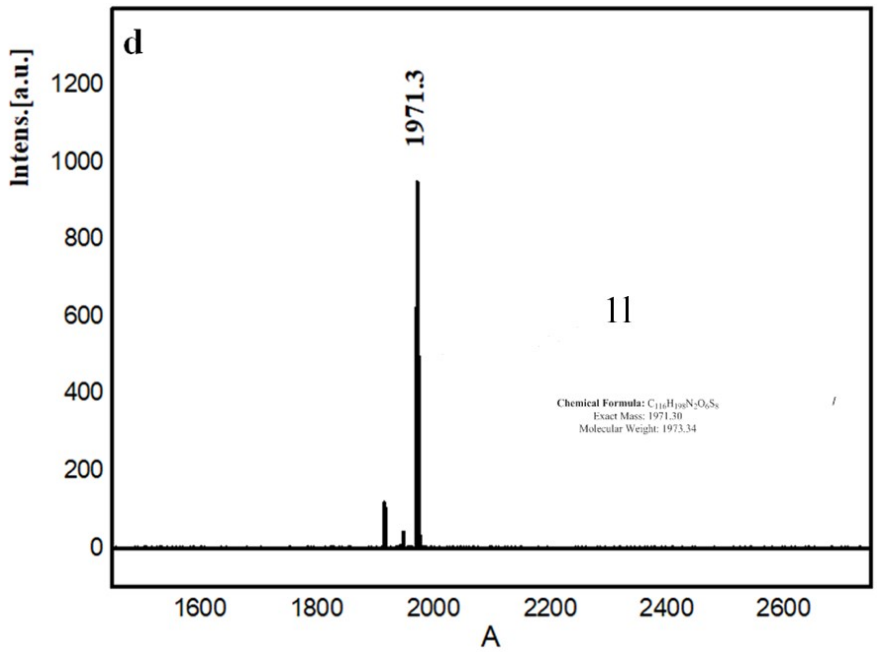

Fig. S19 (a) ^{1}H NMR of the target compound **1j**

(b) ^{13}C NMR of the target compound **1j**

(c) FT-IR of the target compound **1j**

(b) MALDI-TOF-MS of the target compound **1j**

3. Additional data

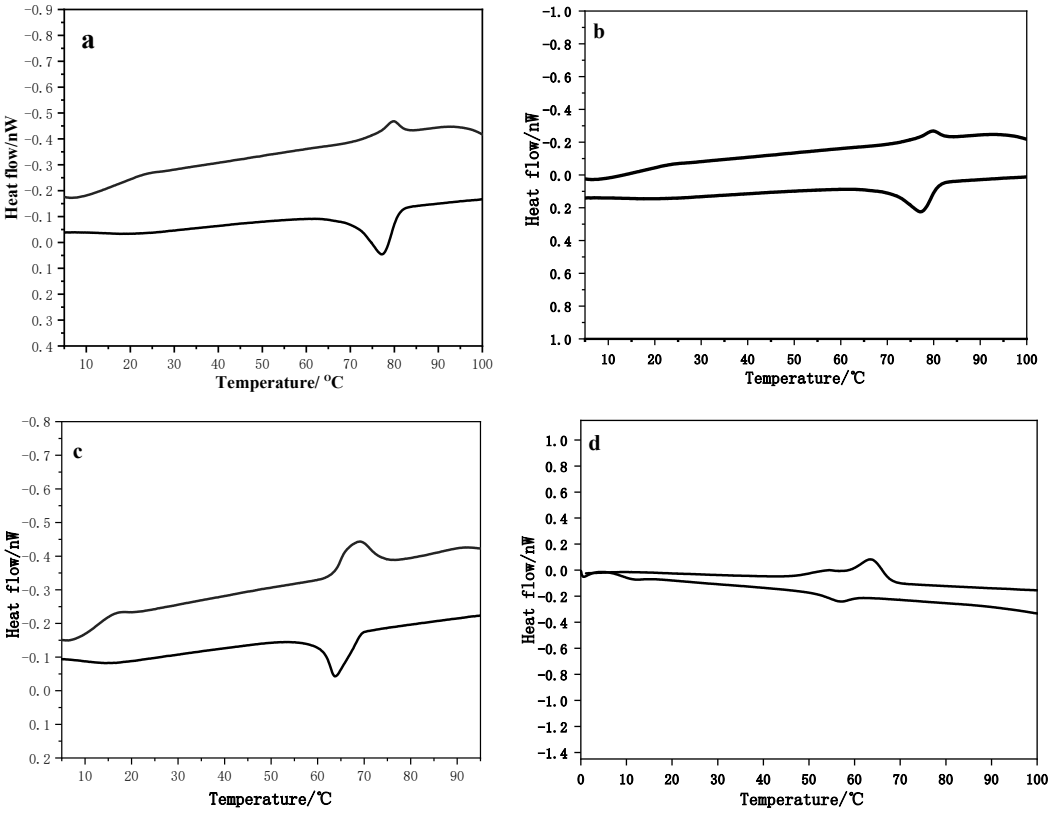

Fig. S20 DSC traces (10 °C/min) recorded during the second heating and the second cooling scan of compounds **1e(a), 1f(b), 1i(c), 1k(d)**

Table S1 Phase transition temperature and enthalpy changes of **1e, 1f, 1i, 1k** determined by DSC in the second cooling scan[a]

Compd	Transition temperature(°C) and enthalpy changes (J g-1), Heating cycle/Cooling cycle	ΔT^b /°C	T_d [c]/°C
1e	g 11.4 S_A 75.8 (1.55) I/I 77.2 (7.5) S_A 9.9 g	64.4	263
1f	g 18 .1 S_A 77.5 (2.7) I/I 72.5 (3.8) S_A 17.2g	59.5	267
1i	g 9.4 S_A 63.6 (3.7) I/I 60.3 (3.2) S_A 6.8g	53.2	262
1j	g 9.2 S_A 66.4 (4.9) I/I 64.6 (4.4) S_A 6.4g	57.2	271
1k	g 6.7 S_A 59.5 (1.7) I/I 52.6 (4.4) S_A 6.3g	53.8	268

[a] g=glass state, S_A=smectic A, , I=isotropic.

[b] Mesophase temperature ranges on heating cycle.

[c] Temperature at which 5% weight loss occurred.

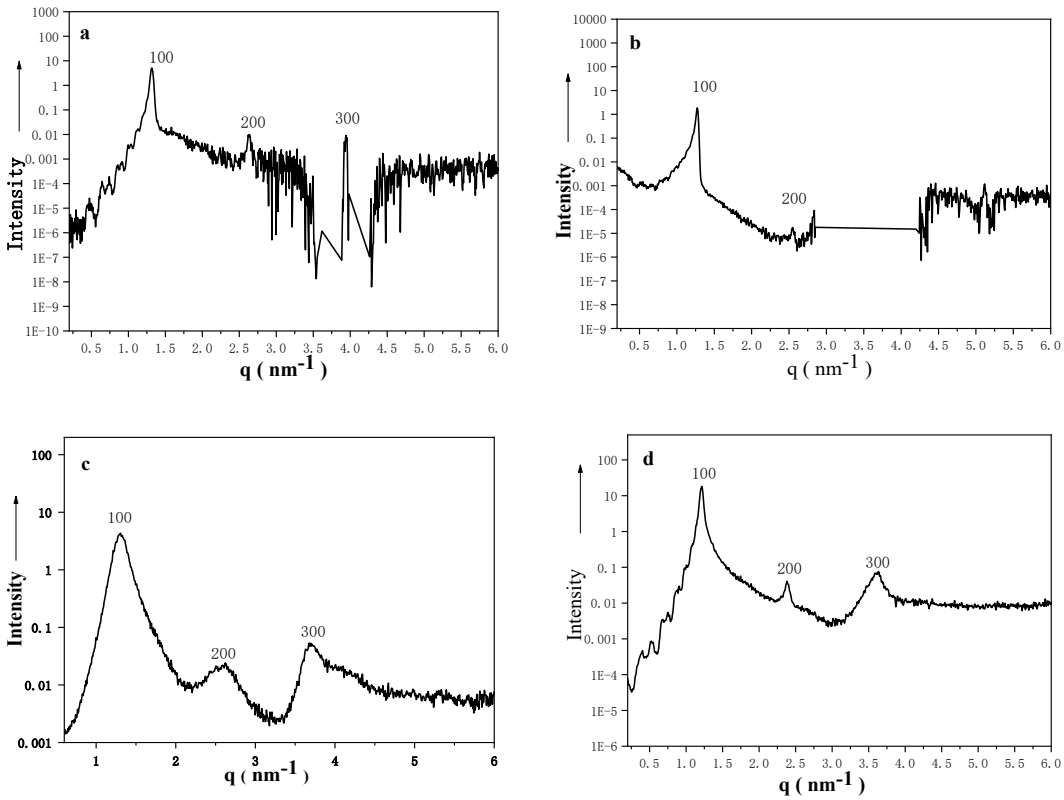

Fig. S21 SAXS patterns along with possible assembled structures (inset) of compound **1e** (a)**,** **1f**(b), **1i**(c), **1h**(d) at 40 ºC on cooling from the isophase.

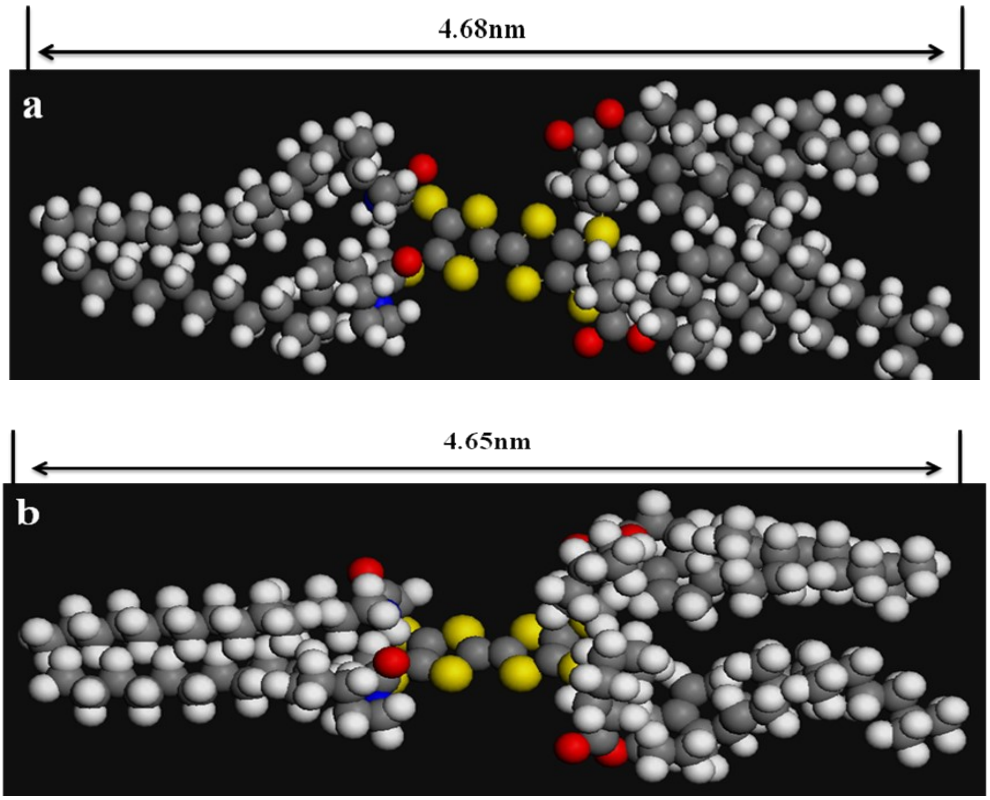

Fig. S22 CPK model of **1k(a)** and **1h(b)**

Table S2 SAXS data for the selected compounds

Compd	Measured spacing/nm		
1e	4.83(100)	2.41(200)	1.61(300)
1f	4.94(100)	2.47(200)	-(300)
1i	4.86(100)	2.42(200)	1.67(300)
1j	5.23(100)	2.64(200)	1.74(300)
1k	5.21(100)	2.63(200)	1.73(300)

Table S3 Gelation properties of **1a–d** in various solvents

Solvent	**1a**	**1b**	**1c**	**1d**
Cyclohexane	TG(7.6mg/mL)	TG(5.8mg/mL)	TG(3.6mg/mL)	TG(1.7mg/mL)
n-hexane	IS	IS	IS	OG(5mg/mL)
Benzene	S	S	S	S
Toluene	S	S	S	S
Chlorobenzene	S	S	S	S
Xylene	S	S	S	S
Carbon tetrachloride	S	S	S	S
Isopropanol	sS	P	IS	OG(5.5mg/mL)
Ethyl acetate	OG(21.4mg/mL)	OG(11mg/mL)	OG(7.1mg/mL)	OG(7.3mg/mL)
Tetrahydrofuran	S	S	S	S
Methanol	IS	IS	IS	IS
Ethanol	IS	IS	IS	sS
Acetonitrile	IS	IS	IS	IS
Diethyl ether	IS	IS	IS	sS
DMF	sS	P	TG(11.7mg/mL)	TG(7.3mg/mL)
DMSO	sS	P	P	P
Acetone	IS	IS	TG(18mg/mL)	IS
1,2-Dichloroethane	S	S	S	S
Cyclohexanol	sS	TG(18mg/mL)	OG(16.9mg/mL)	TG(3.1mg/mL)
N-butyl alcohol	TG(15.4mg/mL)	OG(11mg/mL)	TG(6.36mg/mL)	OG(16.9mg/mL)
Methylcyclohexane	S	S	S	S
Dichloromethane	S	S	S	S

OG=opaque gel; TG=transparent gel; PG=part gel; P=precipitation; S=soluble; IS=insoluble; sS=slight soluble. CGC=the critical gelation concentrations(mg/mL) at room temperature.

Table S4 Gelation properties of **1e–h** in various solvents

Solvent	**1e**	**1f**	**1g**	**1h**
Cyclohexane	TG(1.7mg/mL)	TG(2.7mg/mL)	TG(2.6mg/mL)	TG(1.0mg/mL)
n-hexane	IS	IS	sS	OG(3.9mg/mL)
Benzene	TG(12.0mg/mL)	TG(18.2mg/mL)	TG(20.0mg/mL)	S
Toluene	TG(7.7mg/mL)	TG(14.1mg/mL)	TG(19.0mg/mL)	S
Chlorobenzene	S	S	S	S
Xylene	TG(5.1mg/mL)	TG(12.4mg/mL)	TG(13.0mg/mL)	S
Carbon tetrachloride	TG(14.7mg/mL)	TG(13.8mg/mL)	S	S
Isopropanol	P	P	OG(9.0mg/mL)	P
Ethyl acetate	IS	IS	OG(7.1mg/mL)	P
Tetrahydrofuran	S	S	S	S
Methanol	IS	IS	IS	IS
Ethanol	IS	sS	IS	sS
Acetonitrile	IS	IS	IS	IS
Diethyl ether	IS	IS	IS	sS
DMF	OG(5.8mg/mL)	IS	OG(10.5mg/mL)	OG(8.5mg/mL)
DMSO	OG(28.8mg/mL)	IS	P	P
Acetone	IS	IS	P	IS
1,2-Dichloroethane	TG(8.8mg/mL)	TG(8.8mg/mL)	S	TG(7.8mg/mL)
Cyclohexanol	TG(10.5mg/mL)	TG(10.0mg/mL)	TG(10.5mg/mL)	TG(9.5mg/mL)
N-butyl alcohol	OG(3.1mg/mL)	IS	OG(18mg/mL)	OG(4.8mg/mL)
Methylcyclohexane	S	S	S	S
Dichloromethane	S	S	S	S

OG=opaque gel; TG=transparent gel; PG=part gel; P=precipitation; S=soluble; IS=insoluble; sS=slight soluble. CGC=the critical gelation concentrations(mg/mL) at room temperature.

Table S5 Gelation properties of **1i–l** in various solvents

Solvent	**1i**	**1j**	**1k**	**1l**
Cyclohexane	TG(2.3mg/mL)	TG(3.3mg/mL)	TG(9.0mg/mL)	TG(3.8mg/mL)
n-hexane	IS	IS	S	OG(2.5mg/mL)
Benzene	TG(5.4mg/mL)	TG(10.5mg/mL)	S	TG(23.0mg/mL)
Toluene	S	TG(11.0mg/mL)	TG(48.0mg/mL)	TG(19.0mg/mL)
Chlorobenzene	S	S	S	S
Xylene	TG(2.3mg/mL)	TG(10.5mg/mL)	S	TG(23.0mg/mL)
Carbon tetrachloride	TG(4.4mg/mL)	TG(11.4mg/mL)	S	TG(22.0mg/mL)
Isopropanol	P	P	P	OG(8.7mg/mL)
Ethyl acetate	OG(14.0mg/mL)	OG(16.0mg/mL)	P	OG(2.9mg/mL)
Tetrahydrofuran	S	S	S	S
Methanol	IS	IS	IS	IS
Ethanol	IS	sS	IS	sS
Acetonitrile	IS	IS	IS	IS
Diethyl ether	IS	IS	sS	sS
DMF	OG(3.7mg/mL)	P	P	IS
DMSO	OG(24.0mg/mL)	P	P	sS
Acetone	IS	IS	P	sS
1,2-Dichloroethane	TG(2.0mg/mL)	TG(12.0mg/mL)	S	TG(6.5mg/mL)
Cyclohexanol	TG(6.0mg/mL)	OG(11.0mg/mL)	S	TG(1.9mg/mL)
N-butyl alcohol	P	P	P	OG(1.8mg/mL)
Methylcyclohexane	S	S	S	S
Dichloromethane	S	S	S	S

OG=opaque gel; TG=transparent gel; PG=part gel; P=precipitation; S=soluble; IS=insoluble; sS=slight soluble. CGC=the critical gelation concentrations(mg/mL) at room temperature.

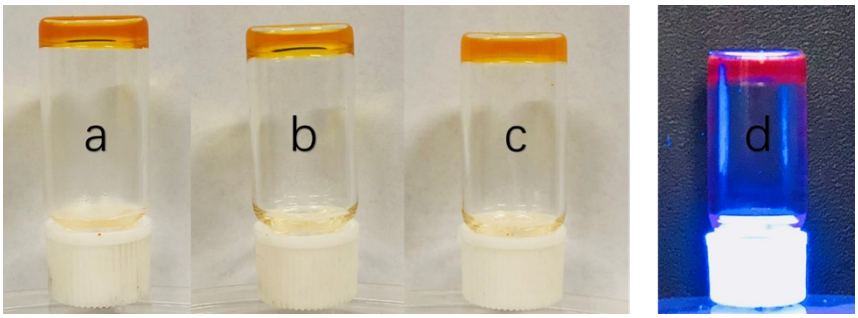

Fig. S23 Photographs of organogel **1b** in different solvents: (a) cyclohexanol; (b) cyclohexane; (c) ethyl acetate; (d) rhodamine B in cyclohexane and the corresponding fluorescent organogel under UV light (wavelength: 365 nm).

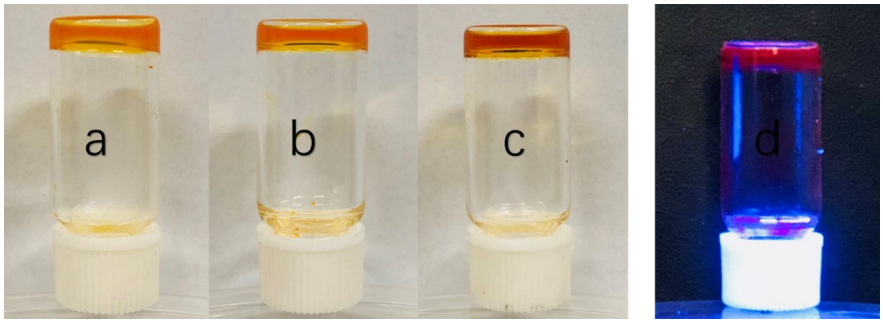

Fig. S24 Photographs of organogel **1f** in different solvents: (a) cyclohexanol; (b) cyclohexane; (c)1,2-dichloroethane; (d) rhodamine B in cyclohexane and the corresponding fluorescent organogel under UV light (wavelength: 365 nm).

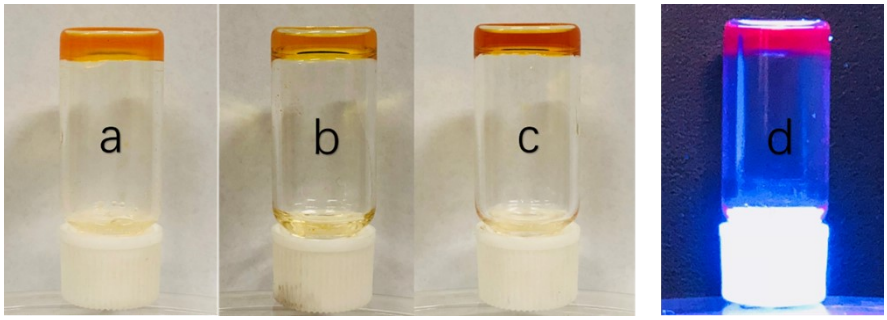

Fig. S25 Photographs of organogel **1j** in different solvents: (a) cyclohexanol; (b) cyclohexane; (c)1,2-dichloroethane; (d) rhodamine B in cyclohexane and the corresponding fluorescent organogel under UV light (wavelength: 365 nm).

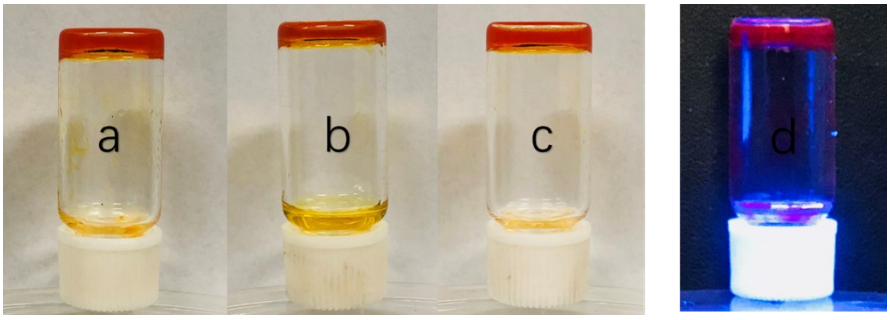

Fig. S26 Photographs of organogel **1k** in different solvents: (a) benzene; (b) toluene; (c) carbon tetrachloride; (d) rhodamine B in cyclohexane and the corresponding fluorescent organogel under UV light (wavelength: 365 nm).

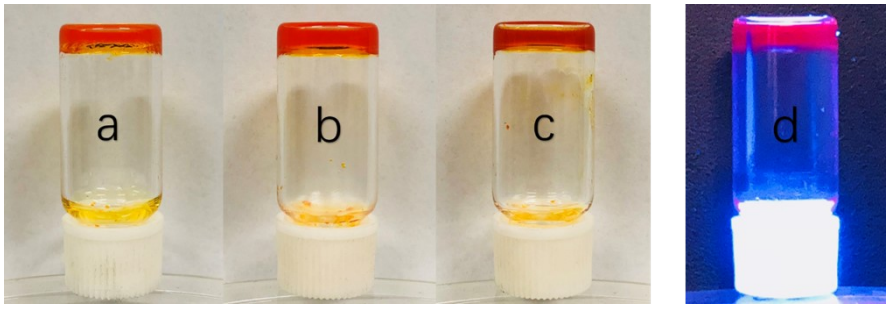

Fig. S27 Photographs of organogel **1l** in different solvents: (a) benzene; (b) xylene; (c) carbon tetrachloride; (d) rhodamine B in cyclohexane and the corresponding fluorescent organogel under UV light (wavelength: 365 nm).

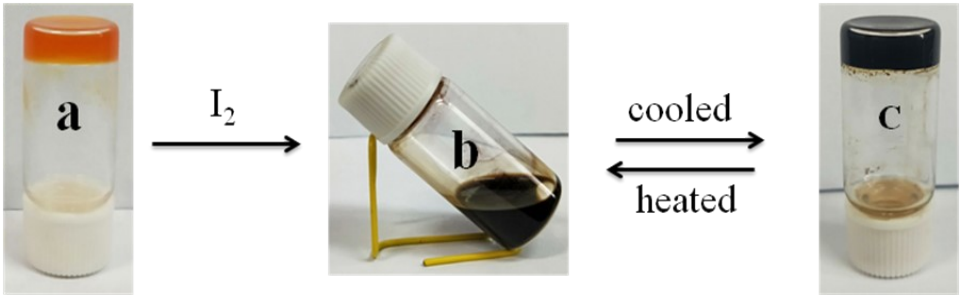

Fig. S28 Tuning the gel formation with the addition of I_2. (a) a cyclohexane organogel of **1b**; (b) a brown solution of the CT complex; and (c) a brow binary gel of the CT complex.

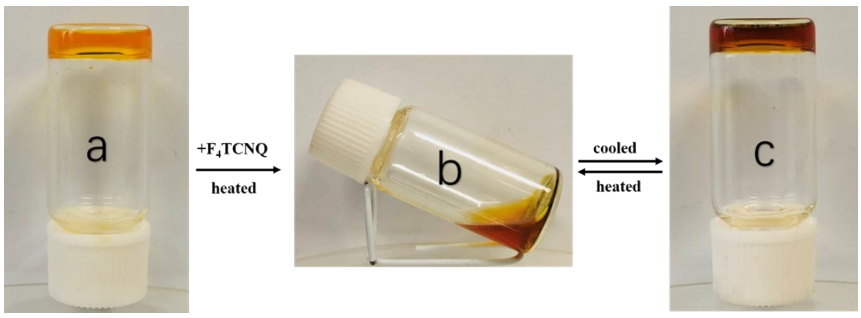

Fig. S29 Tuning the gel formation with the addition of F_4TCNQ. (a) a cyclohexane organogel of **1b**; (b) a brown solution of the CT complex; and (c) a brow binary gel of the CT complex.

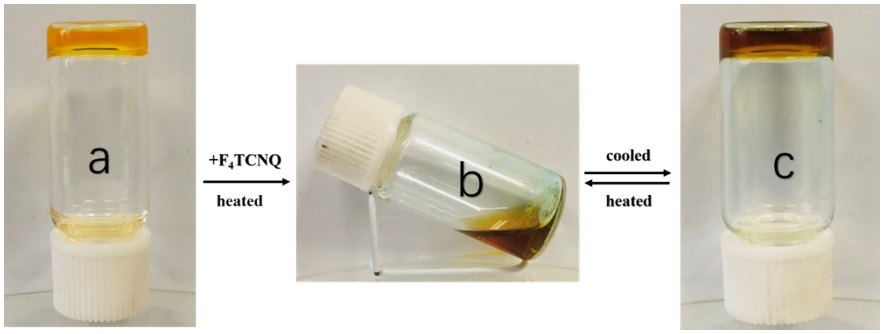

Fig. S30 Tuning the gel formation with the addition of F_4TCNQ. (a) a cyclohexane organogel of **1f**; (b) a dark-brown solution of the CT complex; and (c) a dark-brow binary gel of the CT complex.

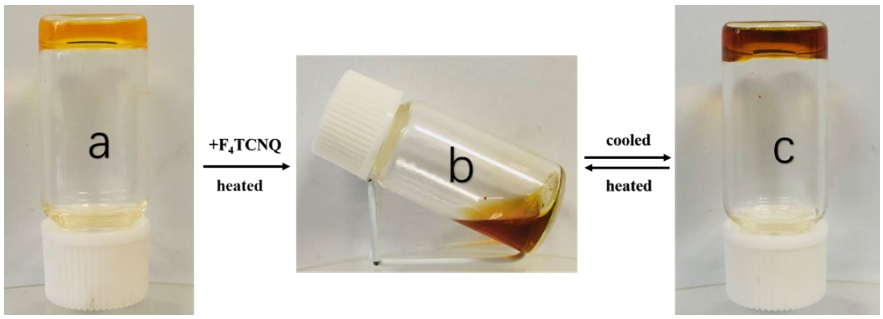

Fig. S31 Tuning the gel formation with the addition of F_4TCNQ. (a) a cyclohexane organogel of **1j**; (b) a brown solution of the CT complex; and (c) a brow binary gel of the CT complex.

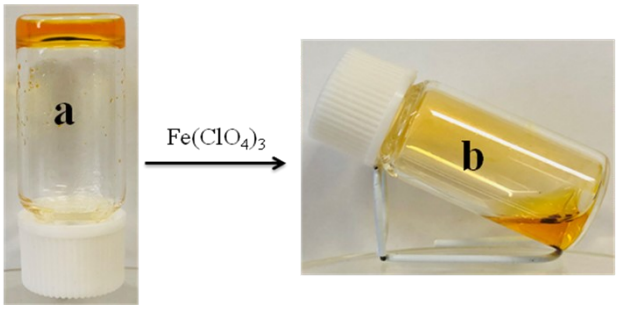

Fig. S32 Tuning the gel formation with the addition of Fe^{3+}. (a) a cyclohexane organogel of **1j**; (b) a dark brown suspension gel of the CT complex.

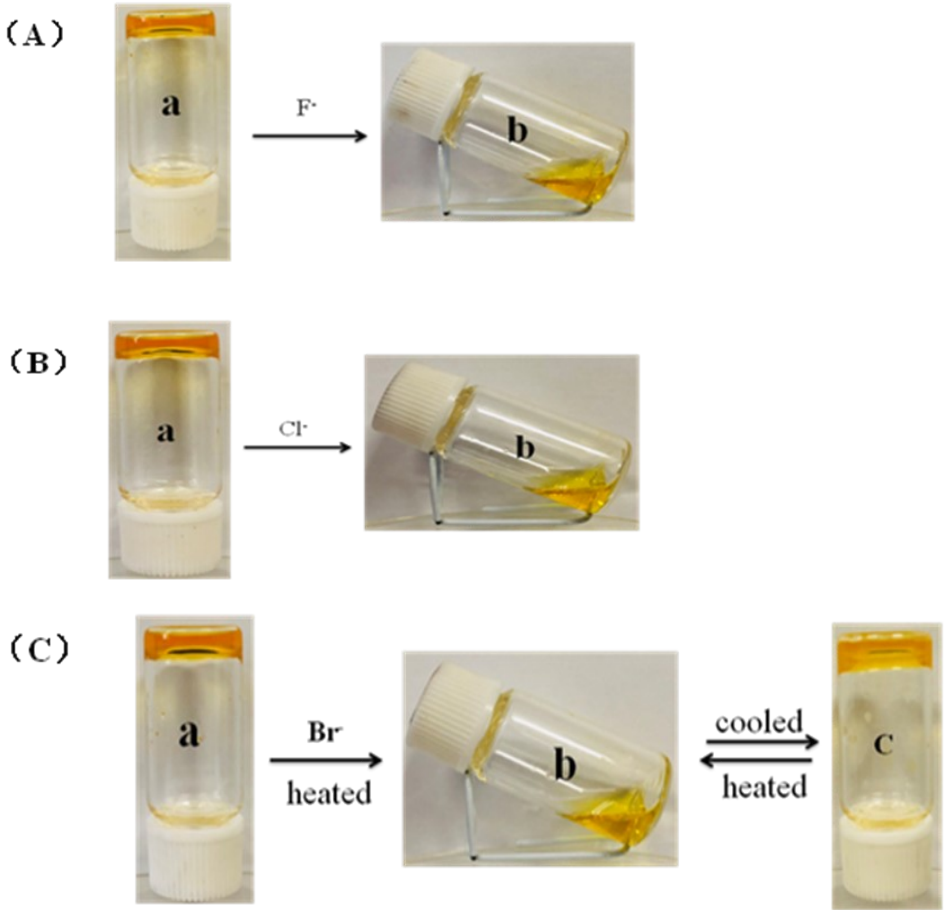

Fig. S33 Photographs of native gel of 1 in cyclohexane upon the addition of 2.0 equiv of each anion, from top to bottom is native gel (A), F^- (B), Cl^- (C), Br^-.

Table S6 The calculated thermodynamic parameters of gelation

Parameters	**1c**	**1g**	**1k**
δ (lnφ) / δ T	0.05179	0.19625	0.09029
△G (KJ·mol-1·K-1)	-20975.53	-22192.46	-21457.42
△G (KJ·mol-1·K-1)	-43583.27	-153929.10	-70358.76
△S (J·mol-1·K-1)	-71.06	-428.90	-159.73

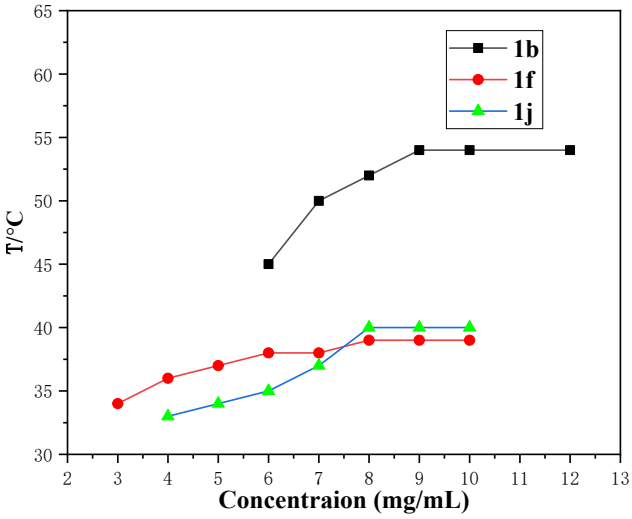

Fig. S34 Plots of T_{gel} versus the concentration of **1b**, **1f**, **1j** in cyclohexane.

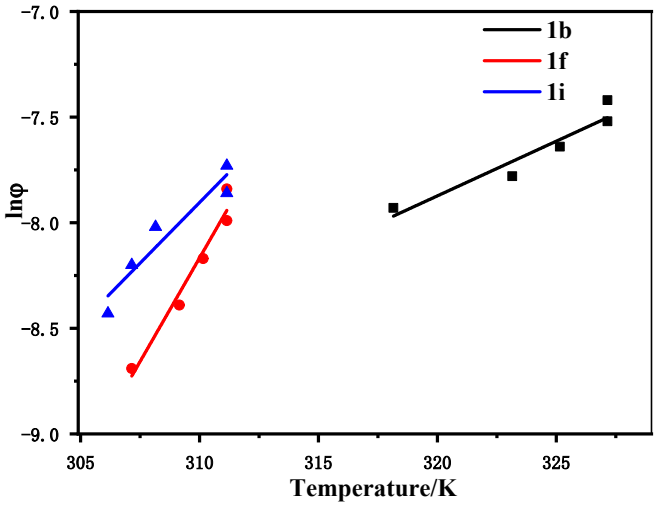

Fig. S35 Plots of lnφ vs. T for organogels of **1b** (■), **1f** (●), **1j**(▲) in cyclohexane.

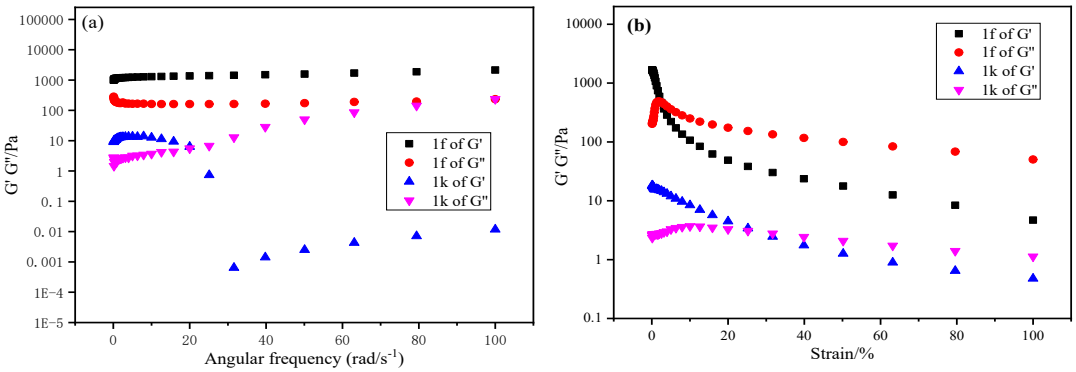

Fig. 36 (a) Frequency dependence of the storage modulus (G') and loss modulus (G'') of **1f** and **1k** gels in cyclohexane. The strain amplitude was 0.1%; (b) amplitude dependence of the storage modulus (G') and loss modulus (G'') of **1f** and **1k** gels in cyclohexane. The frequency was 1 Hz.

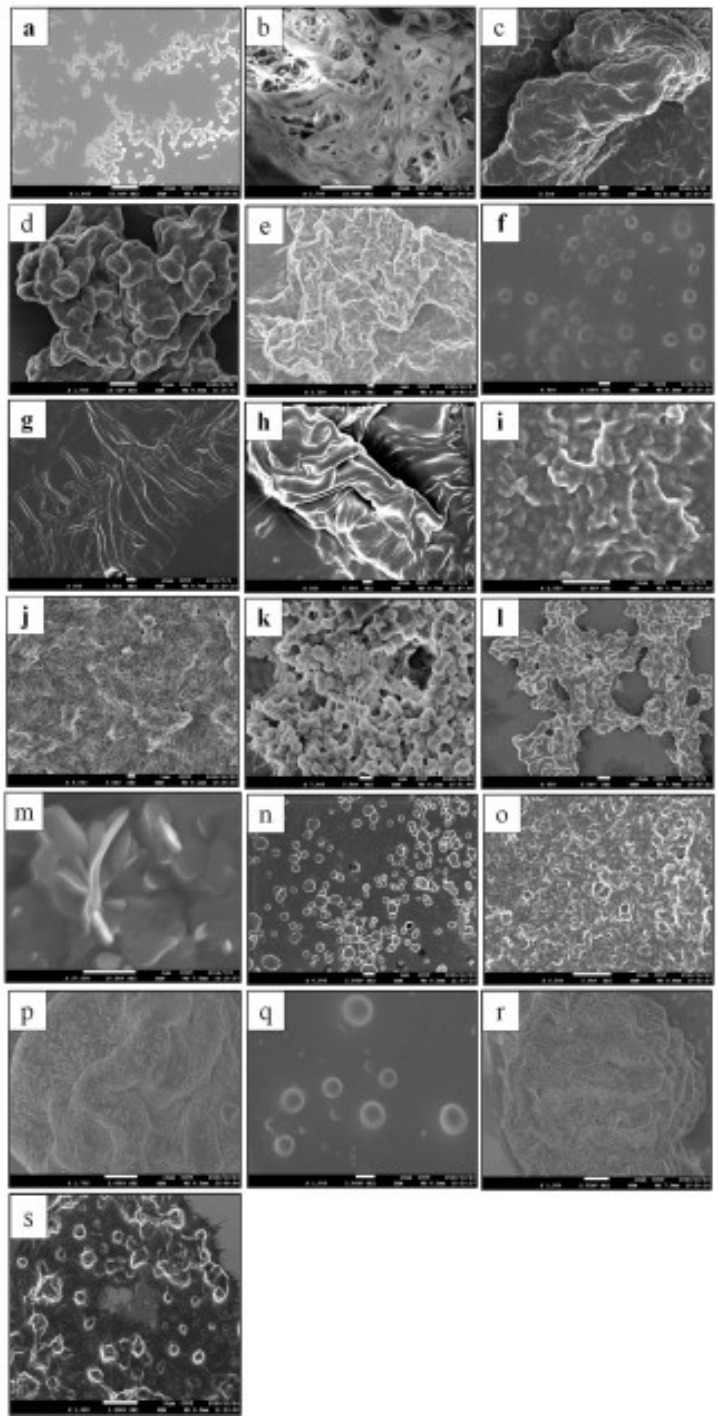

Fig. S37 FE-SEM images of xerogels of **1** in (a) **1a**; (b) **1b** in cyclohexane; (c) **1c** in cyclohexane; (d) **1c** in ethyl acetate; (e) **1c** in n-butyl alchohol; (f) **1f** in cyclohexane; (g) **1f** in benzene; (h) **1f** in p-xylene; (i) **1f** in cyclohexanol; (j) **1g** in DMF; (k) **1h** in DMF: (l) **1l** in cyclohexane; (m) **1j** in dichloromethane; (n) **1k** in cyclohexane; (o) **1l** in dichloromethane; (p) **1l in** benzene; (q) **1l** in cyclohexane; (r) **1l** in methylbenzene; (s) **1l** in isopropanocyclohexanel.

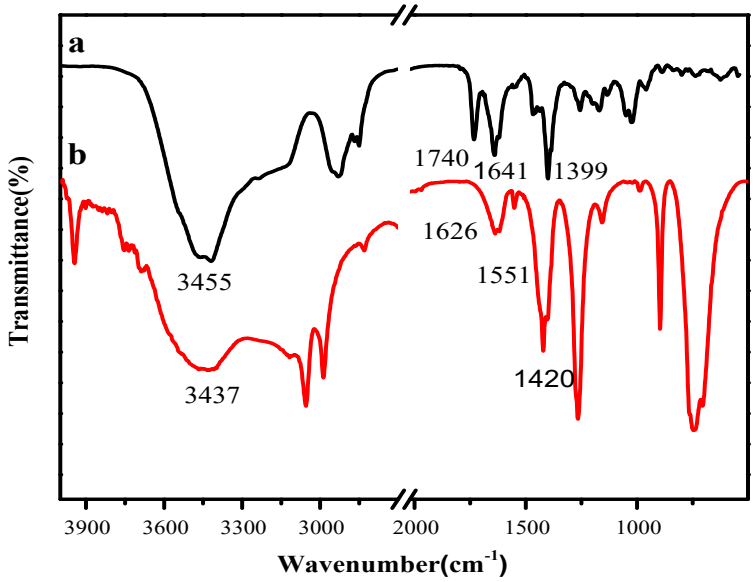

Fig. S38 FT-IR spectra of **1l** in CH_2Cl_2 solution (a), native xerogel of **1l** from toluene (b), native xerogel of **1l** from cyclohexane.

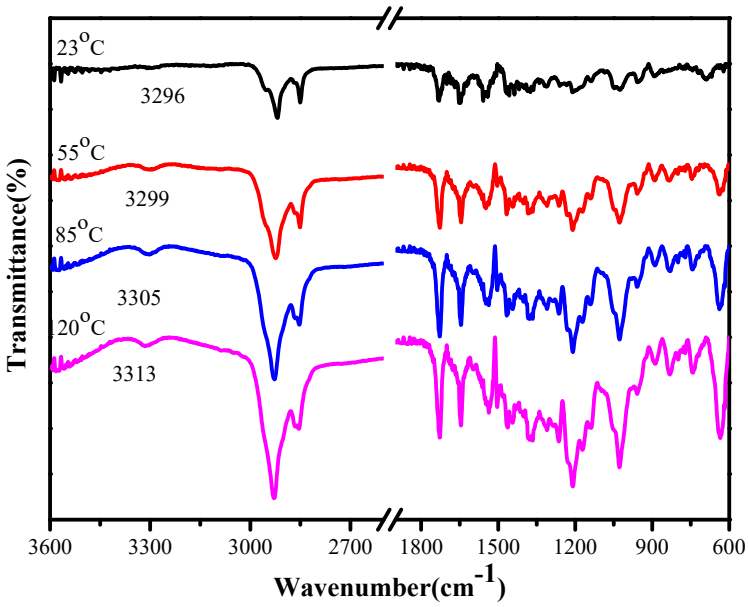

Fig. S39 In situ temperature-dependent FT-IR spectra of xerogel **1l** .

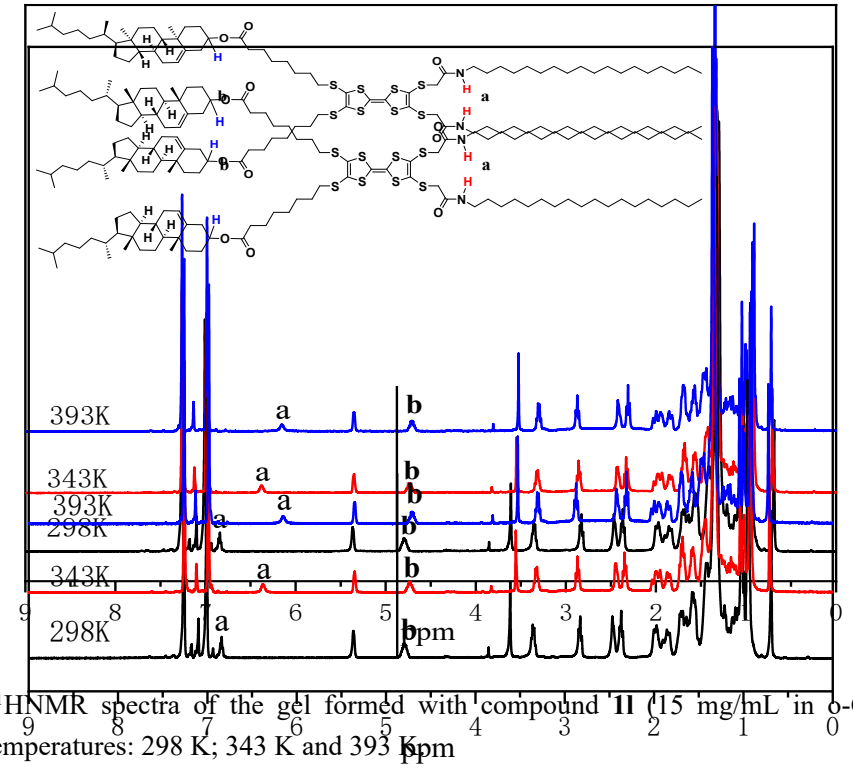

Fig. S40 ^{1}HNMR spectra of the gel formed with compound **1l** (15 mg/mL in o-$C_6D_4Cl_2$) at different temperatures: 298 K; 343 K and 393 K.